

1 **Characterisation of the symbionts in the Mediterranean fruitfly gut**

2

3 Darrington, M.<sup>1\*</sup>, Leftwich, P.T.<sup>1\*</sup>, Holmes, N.A.<sup>1,4</sup>, Friend, L.A.<sup>1</sup>, Clarke N.V.E.<sup>1</sup>, Worsley, S.F.<sup>1</sup>,  
4 Margaritopolous, J.T.<sup>2</sup>, Hogenhout, S.A.<sup>3</sup>, Hutchings, M.I.<sup>1,4</sup> & Chapman, T<sup>^1</sup>

5

6 <sup>1</sup>School of Biological Sciences, University of East Anglia, Norwich Research Park, Norwich, NR4  
7 7TJ, UK.

8 <sup>2</sup>Department of Plant Protection, Institute of Industrial and Fodder Crops, Hellenic Agricultural  
9 Organization–DEMETER, Volos, Greece

10 <sup>3</sup>Department of Crop Genetics, John Innes Centre, Norwich Research Park, NR4 7UH, Norwich,  
11 UK

12 <sup>4</sup>Department of Molecular Microbiology, John Innes Centre, Norwich Research Park, Norwich, NR4  
13 7UH, UK.

14

15 \*Joint first authors

16

17 ORCID: PTL 0000-0001-9500-6592

18 ORCID: TC 0000-0002-2401-8120

19 ORCID: NAH 0000-0002-4979-9680

20 ORCID: SFW 0000-0003-4736-0938

21 ORCID: SAH 0000-0003-1371-5606

22 ORCID: MH 0000-0001-6628-5940

23 ORCID: JM 0000-0002-5893-8400

24 ^Correspondence: [tracey.chapman@uea.ac.uk](mailto:tracey.chapman@uea.ac.uk)

25

26

27 Running head: medfly gut microbiome

28

29 Keywords: *Klebsiella oxytoca*, symbiont, paratransgenesis, 16S rDNA sequencing.

30

31 **Abstract**

32 Symbioses between bacteria and their insect hosts can range from very loose associations through  
33 to obligate interdependence. While fundamental evolutionary insights have been gained from the in-  
34 depth study of obligate mutualisms, there is increasing interest in the evolutionary potential of flexible  
35 symbiotic associations between hosts and their gut microbiomes. Understanding relationships  
36 between microbes and hosts also offers the potential for exploitation for insect control. Here, we  
37 investigate the gut microbiome of a global agricultural pest, the Mediterranean fruitfly (*Ceratitis*  
38 *capitata*). We used 16S rRNA profiling to compare the gut microbiomes of laboratory and wild strains  
39 raised on different diets and from flies collected from various natural plant hosts. The results showed  
40 that medfly guts harbour a fairly simple microbiome, primarily determined by the larval diet in both  
41 wild and laboratory flies. However, regardless of the laboratory diet or natural plant host on which  
42 flies were raised, *Klebsiella* spp dominated the medfly microbiomes and resisted removal by  
43 antibiotic treatment. We sequenced the genome of the dominant putative *Klebsiella* spp (designated  
44 'Medkleb') isolated from the gut of the Toliman wild type fruitfly strain. Genome-wide ANI analysis  
45 placed Medkleb within the *K. oxytoca* / *michiganensis* group. Molecular, sequence and phenotypic  
46 analyses supported its identity as *K. oxytoca*. Medkleb has a genome size (5 825 435 bp) which is  
47 1.6 standard deviations smaller than the mean genome size of free-living *Klebsiella* spp, and lacks  
48 some genes involved in environmental sensing. Moreover, the Medkleb genome contains at least  
49 two recently acquired unique genomic islands as well as genes that encode pectinolytic enzymes  
50 capable of degrading plant cell walls. This may be advantageous given that the medfly diet includes  
51 unripe fruits containing high proportions of pectin. These results suggest that the medfly harbours a  
52 commensal gut bacterium that may have developed a mutualistic association with its host and  
53 provide nutritional benefits.

## 54 Introduction

55 All eukaryotic organisms host bacteria (McFall-Ngai et al 2013) and some of the best-studied  
56 associations are those that occur between insects and bacteria (Moran et al 2008; McCutcheon and  
57 Moran 2011; Moran and Bennett 2014). The majority of microbe-insect interactions are temporary  
58 associations. However, some bacteria and insects retain persistent associations over evolutionary  
59 time and have evolved co-dependence (Moran et al 2008). In the most extreme examples, these  
60 associations have persisted for millions of years and represent intimate co-evolutionary relationships  
61 (Moran et al 2005; Moran et al 2008).

62

63 Heritable symbioses are one such example and are defined by the direct passage of bacteria from  
64 insects to progeny, usually via maternal transmission (Moran et al 2008). These symbioses can be  
65 facultative or obligate (Moran et al 2008). Over evolutionary time, facultative symbionts may lose  
66 genes that facilitate life in varied environments (Moran and Bennett 2014). A transition to  
67 evolutionary interdependence with hosts can often be identified by reduced genome size and  
68 reduced GC content (Shigenobu et al 2000; van Ham et al 2003; Wu et al 2006; Hansen et al  
69 2011; Bennett and Moran 2013; Husnik et al 2013). Novel loci can also be acquired via lateral  
70 gene transfer or loci deleted through genome reduction (Ochman et al 2000; Ochman and Davalos  
71 2006). Mutualistic benefits provided to insects by bacteria include synthesis of nutrients (Sabree et  
72 al 2013; Storelli et al 2018; Sinotte et al 2018), carotenoids (Sloan and Moran 2012), and  
73 antipredation molecules (Oliver et al 2003; Sinotte et al 2018). Heritable symbionts include  
74 “reproductive parasites” that enhance their fitness by distorting the sex ratios of the hosts’ offspring  
75 (Hurst and Frost 2015). For example, male *Zyginidia pullulan* leafhopper embryos are feminised by  
76 maternally-inherited *Wolbachia* bacteria (Negri et al 2009). Feminisation benefits *Wolbachia*,  
77 because these bacteria preferentially reside within ovaries and therefore are transmitted across  
78 generations at higher frequency (Negri et al 2009). The *Buchnera* symbionts of aphids have been  
79 extensively studied and represent an example of an advanced obligate mutualism (Shigenobu et al  
80 2000; Tamas et al 2002; van Ham et al 2003). *Buchnera spp* have been associated with aphids for  
81 approximately 100M years (Von Dohlen and Moran 2000) and provide the host with essential  
82 amino acids (Shigenobu et al 2000). There is an increasing body of research into the identities and  
83 potential roles of diverse symbionts found across many different taxa (de Souza et al 2009; Weiss  
84 and Kaltenpoth 2016; Holmes et al 2016; Whitten and Dyson 2017; Ballinger and Perlman 2017;  
85 Anbutsu et al 2017; Heine et al 2018) including those that are only loosely associated with their  
86 hosts, such as the gut symbionts of fruitflies that are the focus of this study.

87

88 There are many examples of studies in which the culturable and non-culturable members of gut  
89 microbiome communities have been characterised via sequencing of specific regions of the  
90 bacterial 16S rDNA. These works show that dipteran gut microbiomes are often relatively stable  
91 and simple (Chandler et al 2011; Gould et al 2018; Deguenon et al 2019) and can in some species

92 be strongly influenced by host diet (Chandler et al 2011; Woruba et al 2019). For example, the gut  
93 microbiome of *Drosophila melanogaster* is consistently formed by a core of five species:  
94 *Lactobacillus plantarum*, *Lactobacillus brevis*, *Acetobacter pasteurianus*, *Acetobacter tropicalis* and  
95 *Acetobacter orientalis* (Gould et al 2018). These simple microbiomes appear to contain bacteria  
96 that reliably colonise the gut, suggesting the potential for hosts to actively regulate their gut  
97 microbiomes (Lhocine et al 2008; Bosco-Drayon et al 2012; Lindberg et al 2018) and gain potential  
98 benefits from doing so (Gould et al 2018). The five core members of the *D. melanogaster* gut  
99 microbiome metabolise lactic acid and acetic acid, which may benefit larvae feeding on rotten fruit.  
100 In contrast, the *Tephritidae* family of “true fruit-fly” pests hatch in unripe fruit and the culturable  
101 species within their gut microbiomes are reported to contain pectinolytic bacteria, which could  
102 assist the host in breaking down plant cell walls (Behar et al 2008b; Ben-Yosef et al 2014; Liu et al  
103 2016).

104

105 Manipulation of the co-evolved intimacy of symbionts and hosts via paratransgenesis has the  
106 potential to be used as a novel mode of pest insect control (Durvasula et al 1997; Whitten et al  
107 2016). Gut symbionts have the potential to augment strategies for control as probiotics. For  
108 example, they could boost fitness in insects such as Mediterranean fruitflies (medfly, *Ceratitis*  
109 *capitata*) that are subjected to potentially damaging irradiation as part of sterile insect release  
110 control programmes (Jurkevitch 2011). The potential utility of symbionts to either provide new  
111 routes for pest control or to improve existing technologies (Leftwich et al 2016) has led to  
112 increasing interest in investigating the symbiotic gut microbial communities of key global pests,  
113 such as the medfly (Behar et al 2008a; Behar et al 2008b; Ben Ami et al 2010; Gavriel et al 2011),  
114 which is the focus of investigation here.

115

116 Investigations of culturable gut bacteria in medfly have been predominantly performed using  
117 amplified rDNA restriction analysis (ARDRA). These show that *Klebsiella* spp comprise at least 20-  
118 30% of the larval, pupal and adult medfly gut microbiomes (Behar et al 2008b; Ben Ami et al 2010;  
119 Aharon et al 2013). This has led to the hypothesis that *K. oxytoca* might benefit larval nutrition via  
120 its reported pectinolytic activity against fruit sugars, or due to its ability to fix nitrogen (Behar et al  
121 2008b). 16S rDNA analysis has also been used to show that irradiation can alter the microbiome,  
122 and particularly diminishes the relative contribution of *Klebsiella* spp (Ben Ami et al 2010).  
123 Subsequent reintroduction of *K. oxytoca* to irradiated flies significantly reduced mating latency in  
124 comparison to males fed sterile diet (Ben Ami et al 2010), suggesting a potential host fitness benefit.

125

126 Although the culturable species within medfly microbiomes have been described, with *Klebsiella* spp  
127 appearing to be a typical component, many details remain unknown. For example, we do not yet  
128 know the contribution of non-culturable species to both laboratory and wild medfly, whether  
129 microbiomes are stable, whether *Klebsiella* spp have the capability to confer a direct fitness benefit

130 to the medfly, and the extent to which *Klebsiella* is heritable. Behar et al. (Behar et al 2008a) suggest  
131 that a gut symbiont identified as *K. oxytoca* is heritable and can be transmitted during oviposition.  
132 However, *K. oxytoca* was detected in only 1 of 4 replicate samples (Behar et al 2008a) and the  
133 potential transmission of *K. oxytoca* during oviposition could not be ruled out. Recovery of GFP  
134 labelled *Klebsiella* bacteria in the guts of offspring of mothers into which those bacteria were  
135 experimentally introduced provides stronger evidence of vertical transmission (Lauzon et al 2009),  
136 though the relative importance of this mechanism is not yet clear. In terms of fitness benefits, Gavriel  
137 et al. (Gavriel et al 2011) experimentally depleted the microbiome of male medflies by using  
138 irradiation and fed males with a diet either containing *K. oxytoca* (*pro*) or a sterile diet (*ster*). *pro*  
139 outcompeted *ster* flies for matings, and females mated to *pro* males were less inclined to re-mate.  
140 These data suggest that *Klebsiella* spp could confer host benefits (Behar et al 2008b; Ben Ami et al  
141 2010; Gavriel et al 2011), though it is not yet clear whether this occurs in the natural context.

142

143 Here we compared the culturable and non-culturable gut microbiomes of wild-collected adult  
144 medflies from a range of different wild hosts, with those of the Toliman wild type laboratory strain  
145 reared on a range of different larval diets in the presence and absence of antibiotics. We conducted  
146 long-read genome sequencing and analysis of the genome of the dominant, putative *K. oxytoca*  
147 (hereafter “Medkleb”) spp extracted from the adult gut of Toliman wild type individuals. This was  
148 done to confirm the phylogenetic placement of Medkleb and to interrogate the genome for features  
149 characteristic of a nascent evolutionary interdependence with its medfly host. We assembled and  
150 annotated the Medkleb genome sequence and tested for signatures of facultative transition, i.e. a  
151 reduction in genome size or GC content (Moran et al 2008; McCutcheon and Moran 2011; Moran  
152 and Bennett 2014). We conducted comparisons between Medkleb and other *Klebsiella* spp to reveal  
153 phenotypes that might potentially facilitate a mutualistic relationship, or indicate restrictions to the  
154 environments in which Medkleb might live. We investigated tests of phenotypic features by testing  
155 whether Medkleb had the capacity to synthesise secondary metabolites, and by conducting direct  
156 biochemical tests for pectinolytic activity.

157

## 158 **Materials and Methods**

159

### 160 **1. Toliman Wild type strain**

161 To directly test the effect of different dietary carbohydrates on the gut microbiome, we raised three  
162 replicate samples each of individuals from the Toliman wild type strain on different larval diets. This  
163 strain originated from Guatemala and has been reared in the laboratory since 1990. Our Toliman  
164 colony has been maintained in non-overlapping generations in a controlled environment room  
165 (humidity 50± 5%, temperature 25± 0.5°C) on a 12:12 light:dark cycle for over 30 generations  
166 (Leftwich et al 2017). Under this regime, larvae are raised on a sugar-yeast-maize medium (1% agar,  
167 7.4% sugar, 6.7% maize, 4.75% yeast, 2.5% Nipagin (10% in ethanol), 0.2% propionic acid) and

168 adults are given *ad libitum* access to sucrose-yeast food; 3:1 w/w sugar/ yeast hydrolysate, and  
169 water.

## 170 **2. Generation of laboratory and wild-derived gut microbiome samples**

### 171 *(i) Effect of the larval diet on the adult microbiome in the Toliman wild type*

172 To generate the samples of wild type flies raised on different diets ( $\pm$  antibiotics) for subsequent gut  
173 dissection and 16S rRNA amplicon sequencing of the gut microbiome, Toliman flies were cultured  
174 from eggs collected over a 24h period placed in one of four larval diet treatments. Three of these  
175 diets provided varying carbohydrate levels and sources, while maintaining the same yeast (~protein)  
176 level: 1) Sucrose High Protein (SHP), 2) Glucose & 3) Starch. The fourth diet had a sucrose  
177 carbohydrate base but only 60% of the yeast content: Sucrose Low Protein, SLP (Table S1). We  
178 included Propionic acid as a food preservative (Leftwich et al 2018). All diet manipulations were done  
179 in the presence and absence of antibiotics. For the antibiotic treatments, each larval diet contained  
180 a final concentration of 100 $\mu$ g/ml kanamycin, 200  $\mu$ g/ml ampicillin, 200  $\mu$ g/ml streptomycin, 50  $\mu$ g/ml  
181 chloramphenicol, 100 $\mu$ g/ml apramycin, 100  $\mu$ g/ml hygromycin and 200  $\mu$ g/ml tetracycline.  
182 Approximately 500 eggs were placed on 100 mL of the appropriate diet in a glass bottle. When third  
183 instar larvae started to “jump” from the larval medium, the bottles were laid horizontally on sand and  
184 pupae allowed to emerge for seven days. Pupae were then sieved from the sand and held in 9 mm  
185 petri dishes until adult eclosion.

### 186 *(ii) Effect of wild larval diets on the adult microbiome in wild flies under natural conditions*

187 Wild flies were collected at adult eclosion from fallen argan fruit in Arzou, Ait Melloul, Morocco, in  
188 July 2014, from Apricots, Oranges and Grapefruits in Chania, Crete, July-September 2014 and from  
189 Peaches, Oranges and Tangerines in Ano Lechonia, Greece, July-September 2014. All samples  
190 were preserved in 96% ethanol and sent to the UK before gut dissection and DNA extraction for the  
191 16S rRNA amplicon sequencing described below.

## 192 **3. 16S rRNA gene sequencing and bioinformatics analysis of the gut bacteria derived from** 193 **laboratory- and wild- and derived adult medflies.**

194 We analysed the composition of the gut microbiomes in the dissected guts of the laboratory and  
195 wild-derived flies describe above, by using 16S rRNA amplicon sequencing. Each of the three  
196 biological replicates was a pool of five adult flies (Supplementary Information). Batches of flies were  
197 surface sterilized for 30 seconds in 0.5% sodium hypochlorite (bleach) (Sigma-Aldrich, Cat.  
198 No.7681529) and washed for 30 seconds in sterile 1M PBS (pH 7.4) three times before being  
199 homogenized. 100  $\mu$ L of the third washes were used to check the surface sterilisation efficiency.  
200 There was no microbial growth in any of these tests.

201 We used sterilised pestles to homogenise the surface-sterilised samples inside 2-mL microcentrifuge  
202 tubes, with three freeze/thaw cycles in liquid nitrogen. DNA was extracted using the DNeasy Blood

203 and Tissue Kit (Qiagen) and quality checked using a NanoDrop (Thermoscientific Nanodrop 8000  
204 Spectrophotometer). Approximately 100 ng of DNA per sample was used as the template for PCR  
205 amplification with bacterial universal primers 515F (5'-GTG CCA GCM GCC GCG GTA A-3') and  
206 806R (5'-GGA CTA CHV GGG TWT CTA AT-3) against the 16S rRNA gene. Amplicon sequencing  
207 was performed using paired-end 250 bp V2 chemistry (Illumina MiSeq platform, Earlham Institute  
208 provider).

209 Demultiplexed sequences were obtained using mothur v38.2 (Schloss et al 2009), following their  
210 standard MiSeq operating procedures. Sequence variants were assigned to operational taxonomic  
211 units (OTUs) at a 97% similarity threshold. Taxonomy assignment of OTUs using the Silva database  
212 (release 132). The minimum library sizes per sample were ~17K after passing quality control. All  
213 statistical analyses of amplicon data were conducted in R v3.6.2 (R Core Team 2019) using the  
214 phyloseq (McMurdie and Holmes 2013), vegan (Oksanen et al 2007) and tidyverse (Wickham 2017)  
215 packages. Sequences were rarefied to normalise library sizes. Alpha diversity was estimated using  
216 the Shannon species diversity index. We visualised differences in bacterial community structure  
217 among samples (beta diversity) using non-metric multidimensional scaling (NMDS) plots of Bray-  
218 Curtis distances and performed multivariate analysis of variance (PERMANOVA) with 999  
219 permutations on Unifrac distance matrices.

220

#### 221 **4. Genome sequencing of the dominant gut microbiome *Klebsiella* spp symbiont (Medkleb)** 222 **from the Toliman wild type**

223 We investigated the identity of the recurrent *Klebsiella* spp bacterial symbiont through isolation of  
224 culturable *Klebsiella* spp. colonies from the Toliman strain.

225 (i) *Clonal isolation.* Clonal isolates of *Klebsiella* spp obtained from individuals of the Toliman wild  
226 type strain were made by taking surface sterilized, homogenised samples from adults reared under  
227 the standard conditions described above and plating them onto Simmon's Citrate LB Agar (with  
228 bromothymol blue as a colour indicator). This is a substrate recommended for the isolation of  
229 *Klebsiella oxytoca* and *K. pneumoniae* (Simmons 1926). Culture plates were made from 15 biological  
230 replicates of medfly. Cultures were checked for morphological uniformity and their identity confirmed  
231 with PCR amplification with universal bacterial primers 28F and 806R. Thirteen of the 15 isolates  
232 had identical 16S rRNA gene sequences and were BLAST matched to *K. oxytoca* and our most  
233 abundant OTU from 16S rRNA amplicon sequencing. Two isolates contained colonies which BLAST  
234 matched to *Pantoea* spp. We chose a single *Klebsiella* spp colony at random for genomic  
235 sequencing, as described below.

236 (ii) *DNA preparation.* The single clonal isolate selected for genome sequencing was streaked onto  
237 LB media (15g/L Agar; 5g/L NaCl; 5g/L yeast extract; 1.5g/L glucose; 10g/L tryptone) and incubated  
238 overnight at 25°C, then transferred into a 1.5ml microcentrifuge tube containing 1ml of 10% glycerol.

239 The sample was vortexed for 30 secs then centrifuged at 12000 RPM for 10min. Glycerol was then  
240 removed, and the pelleted bacteria re-suspended in 2ml of SET buffer (65% v/v molecular grade  
241 H<sub>2</sub>O (ThermoFisher); 20% v/v Tris (pH8); 5% v/v 5M NaCl; 5% v/v 10% SDS; 5% v/v 0.5M EDTA)  
242 before transfer to a 15ml falcon tube. 20µg of lysozyme (Sigma) and 0.4µg achromopeptidase  
243 (Sigma) suspended in 40µl of molecular grade water (ThermoFisher) and 0.02µg of RNase  
244 (Fermentas) were added. The sample was mixed gently then incubated at 37°C for 2hrs. 240µL of  
245 10% sodium dodecyl sulphate and 56µL of proteinase K (20mg/ml) were added, before a second  
246 incubation at 56°C for 2hrs, with manual mixing every 30 mins. 800µL of 5M NaCl and 2ml of  
247 chloroform were added and the sample was mixed by hand for 10 mins, before centrifugation at  
248 4000 RPM for 12 mins. The aqueous phase was then carefully transferred to a fresh tube. DNA was  
249 precipitated in 0.6 volume isopropanol, then transferred to a 1.5ml microfuge tube by pipette. DNA  
250 was washed once with 70% ethanol. Ethanol was removed, then 1ml of 70% ethanol was added,  
251 and DNA was left to incubate overnight at 4°C. Ethanol was again removed, and DNA was re-  
252 suspended in 200µL of molecular grade water (ThermoFisher).

253 *(iii) Single molecule real time (SMRT/PacBio) Medkleb genome sequencing.* DNA purity,  
254 concentration, and average fragment size were analysed using Nanodrop (ThermoFisher), Qubit  
255 v2.0 (Invitrogen) and Agilent Tapestation 4200 (Agilent) respectively. DNA was fragmented using a  
256 G-tube (Covaris), and SMRTbell library construction was carried out using a Template Prep Kit 1.0  
257 (PacBio). The library was then size selected to >7kb using the BluePippin system (Sage Science).  
258 Sequencing was carried out on a Pacific Biosciences RSII instrument, using two RSII SMRTcells v3  
259 and P6-C4 chemistry (PacBio, Earlham Institute provider). Each cell was sequenced using a 240-  
260 minute movie, using the Magbead OCPW v1 protocol (PacBio).

261 *(iv) Medkleb genome assembly.* The Medkleb genome was assembled according to the Hierarchical  
262 Genome-Assembly Process (HGAP.3) protocol (Chin et al. 2013) as follows. 1) Mapping – BLASR  
263 (Chaisson et al., 2012) was used to map reads >500bp with a read quality >0.8 to seed reads  
264 >6000bp. 2) Pre-assembly - the Directed Acyclic Graph Consensus (DAGCon) algorithm (Lee et al  
265 2002) was used to produce a consensus sequence based on BLASR mapping. DAGCon then  
266 trimmed the consensus, producing an error-corrected pre-assembled read. 3) *de novo* genome  
267 assembly - the overlap-layout-consensus assembler Celera Assembler v8.1 was used to process  
268 the pre-assembled read into a draft assembly. 4) Final consensus - the draft assembly was polished  
269 using the Quiver multiread consensus algorithm (Chin et al 2013). 5) The final consensus sequence  
270 was then manually trimmed to circularise the genome and place the stop codon (TGA) of the *dnaA*  
271 gene at the 5' terminus.

272 *(v) Medkleb genome quality control.* An estimated Quiver quality value (QV) for the Medkleb final  
273 consensus genome was provided (Earlham Institute). Genome completeness was estimated with  
274 both benchmarking universal single copy orthologues (BUSCO) software 3.0.0 (Simão et al 2015),  
275 and CheckM (Parks et al 2015). The *Enterobacteriales* order and *Enterobacteriaceae* family were



276 used as reference datasets for BUSCO and CheckM analyses respectively. Genome contamination  
277 was estimated with CheckM, and mlplasmids (Arredondo-Alonso et al 2018) was used to classify  
278 contigs as either chromosomal or plasmid DNA. The *Klebsiella pneumoniae* support-vector machine  
279 (SVM) model was utilised for the analysis, with minimum posterior probability specified at 0.7 and  
280 minimum contig length at 1,000nt.

281 (vi) *Annotation and genome mapping*. Coding sequences within the Medkleb chromosomal DNA and  
282 plasmids, were called with the Prodigal algorithm (Hyatt et al 2010). Gene calls were then annotated  
283 with Classic-RAST (Overbeek et al 2014). Ribosomal RNAs (rRNAs) and transfer RNAs (tRNAs)  
284 were called and annotated with Classic-RAST. Circular maps were created for the Medkleb  
285 chromosomal DNA and plasmids using DNAplotter (Carver et al 2009).

## 286 **5. Phylogenetic analyses of the Medkleb *Klebsiella* gut symbiont genome sequence**

287 (i) *16s rRNA gene sequence analyses*. The Medkleb genome was searched for regions homologous  
288 to the 16S rRNA gene sequence of *K. oxytoca* strain ATCC 13182 (NR\_118853.1) with BLASTn  
289 (Altschul et al 1997). The region with greatest homology to NR\_118853.1 (nts 341370-342821) was  
290 then parsed with RNAmmer 1.2 (Lagesen et al 2007) which predicts ribosomal genes. Sixty-one 16S  
291 rRNA gene nucleotide sequences representing 60 *Klebsiella* strains, *Pseudomonas aeruginosa*  
292 strain JB2 and a putative Medkleb 16S sequence were used to create a phylogeny with the SILVA  
293 ACT web app (Pruesse et al 2012). Where possible, non-redundant sequences were extracted from  
294 the SILVA rRNA gene database (Quast et al 2013). All sequences were almost complete (>1400bp)  
295 and met the standard operating procedure for phylogenetic inference (SOPPI) quality criteria set out  
296 by Peplies et al. (Peplies et al 2008). The tree was computed with the FastTree2 maximum likelihood  
297 programme (Price et al 2010) using the GTR evolutionary model and gamma distribution parameters  
298 (Yang 1994). The resulting phylogeny was constructed with FigTree 1.4.3 (Rambaut and Drummond  
299 2009).

300 (ii) *Average Nucleotide Identity (ANI) analyses*. 35 RefSeq whole genome entries extracted from the  
301 NCBI database (Geer et al 2010), representing four *Klebsiella* species, were used to calculate a  
302 hierarchical clustering based on Average Nucleotide Identity (Konstantinidis and Tiedje 2005). The  
303 ANI Calculator (Figueras et al 2014) was used to compute the hierarchy using the BIONJ algorithm  
304 (Gascuel 1997). The tree was constructed with FigTree 1.4.3 (Rambaut and Drummond 2009). To  
305 predict recently acquired Medkleb sequences, the genome was aligned with three closely related  
306 bacteria. Genomes were manually re-ordered to place the *dnaA* stop codon at the 5' terminus.  
307 Synteny was then predicted with progressive Mauve (Darling et al 2010).

308

## 309 **6. Metabolic functions of the Medkleb *Klebsiella* gut symbiont**

310 (i) *Analysis of pectinolytic enzyme activity*. Medkleb's ability to degrade pectin was compared to two  
311 bacterial species identified as positive and negative controls; *Erwinia carotovora* (+ve control) and

312 *Rhizobium leguminosarum* (-ve control) (Wegener 2002; Xie et al 2012). Medkleb bacteria were  
313 cultured in LB broth (5g/L NaCl; 5g/L yeast extract; 1.5g/L glucose; 10g/L tryptone) which had been  
314 stored in 50ml glass bottles and autoclaved prior to use. Each bottle was inoculated with a “loop” of  
315 bacteria and incubated, shaking, in an orbital incubator (New Brunswick Scientific Innova 44) at  
316 200RPM. Medkleb and *Erwinia carotovora* were incubated at 37°C and *Rhizobium leguminosarum*  
317 was incubated at 28°C until optical density was greater than 1.0 at 600nm.

318

319 (ii) *Analysis of presence of pehX and 16S rRNA genes in medkleb.* Bacterial DNA was extracted  
320 using a DNeasy blood and tissue kit (Qiagen) and microbe lysis buffer (MLB) (20 mg/ml of lysozyme  
321 (Sigma) and 5mg/ml of achromopeptidase (Sigma) in 20 mM Tris-HCl, 2 mM EDTA, 1.2% Triton X  
322 (pH 8.0)). 2ml of Medkleb, *Erwinia carotovora* and *Rhizobium leguminosarum* cultures were  
323 centrifuged at 13K RPM for 5 mins, before the supernatants were removed. Pellets were then  
324 homogenised with a clean pestle in liquid nitrogen. 180µl of MLB was added before the sample was  
325 vortexed and incubated at 37°C for two hours. Samples were vortexed every 30 mins during the two-  
326 hour incubation. Buffer AL and ethanol were mixed 1:1 (Buffer ALE) and warmed to 55°C. Each  
327 sample had 400µl of warm Buffer ALE added before being immediately vortexed for 10-15 secs.  
328 Samples were transferred to a spin column and centrifuged at 8000RPM for 60 secs. 500µl of Buffer  
329 AW1 was added and the sample was centrifuged again at 8000RPM for 60 secs. 500µl of Buffer  
330 AW2 was added and the samples were centrifuged at 13 000 RPM for 4 mins. 35µl of warm Buffer  
331 AE (60°C) was added to the centre of the spin membrane and the samples were centrifuged at  
332 6000RPM for 60 secs. DNA purity and concentration were measured using a Nanodrop  
333 (ThermoFisher). The *K. oxytoca* polygalacturonase gene pehX (AY065648.1) was aligned to  
334 genomes of *Klebsiella* bacteria using BLAST (Altschul et al 1997). The presence of  
335 polygalacturonases in genomes of *Klebsiella* bacteria was assessed using the Carbohydrate-Active  
336 enZymes database (CAZy) (Lombard et al 2010).

337

338 (iii) *Polygalacturonase enzyme assay.* Polygalacturonase production of Medkleb, *Erwinia carotovora*  
339 and *Rhizobium leguminosarum* was measured using a DNS colorimetric method (Miller 1959) with  
340 a protocol adapted from Sohail et al. (Sohail and Latif 2016) and Sigma Aldrich protocol EC 3.2.1.1.  
341 Cultures were diluted with LB broth to an optical density of 1.0 at 600nm. Bacteria were then filtered  
342 from culture media with 0.2µm PES syringe filters (ThermoFisher). Treatment reactions (which were  
343 run in triplicate) were set up with 1ml of appropriate filtrate and 1ml of polysaccharide solution (PS)  
344 (0.9% polygalacturonic acid (ThermoFisher) in 0.1M sodium acetate (ThermoFisher) (pH 4.5)), a  
345 blank reaction was set up with 1ml of PS only. All reactions were incubated at 45°C for 30mins before  
346 1ml of colour reagent solution (20% 5.3M potassium sodium tartrate, tetrahydrate in 2M sodium  
347 hydroxide solution; 50% 96 mM 3,5-Dinitrosalicylic acid solution; 30% molecular water  
348 (ThermoFisher)) was added. All reactions were incubated at 100°C for 15 mins, then placed on ice  
349 to cool to room temperature. Once cooled, 12ml of molecular water (ThermoFisher) was added to

350 each reaction, followed by hand mixing. Absorbance at 530nm ( $\Delta A_{530}$ ) was measured using a  
351 spectrophotometer (Biochrom) which had been blanked for air, with the corrected  $\Delta A_{530}$  for  
352 treatment reactions being calculated as:

$$353 \quad \Delta A_{530} (\textit{Treatment reaction}) = \Delta A_{530} (\textit{Treatment reaction}) - \Delta A_{530} (\textit{Blank reaction})$$

354 Units of polygalacturonase in the filtrate were calculated via comparison to a standard curve of  
355 galacturonic acid (Sigma). Standards were made with between 50 $\mu$ l and 1 ml of monosaccharide  
356 solution (MS) (1.8% galacturonic acid (ThermoFisher) in 0.1M sodium acetate (ThermoFisher) (pH  
357 4.5) and topped up to 2ml total volume with molecular water (ThermoFisher). A standard blank was  
358 set up containing 2ml of molecular biology grade water only. 1ml of colour reagent solution was then  
359 added before incubation at 100°C for 15 mins. Standards were placed on ice to cool to room  
360 temperature before 12ml of molecular water was added and  $\Delta A_{530}$  was measured using a  
361 spectrophotometer (Biochrom) which had been blanked for air. The corrected  $\Delta A_{530}$  for standards  
362 was calculated as:  $\Delta A_{530} (\textit{Standard}) = A_{530} (\textit{Standard}) - A_{530} (\textit{Blank})$ . The standard curve was  
363 used to estimate mg of galactose released in treatment reactions with linear regression, and units of  
364 polygalacturonase per ml of filtrate were then calculated as:  $\textit{Units/ml enzyme} = (\textit{mg of galactose}$   
365  $\textit{released})/\textit{ml of filtrate}$ .

366

367 *(iv) Prediction of higher order metabolic functions and secondary metabolites.* The higher order  
368 metabolic functions of genes were predicted using the Kyoto Encyclopaedia of Genes and Genomes  
369 (KEGG) (Kanehisa et al 2016). Secondary metabolites were predicted using antiSMASH 6.0 beta  
370 (Blin et al 2019).

371

372

373 **Results**

374

375 **1. Characterisation of the medfly gut microbiome using amplicon sequencing**

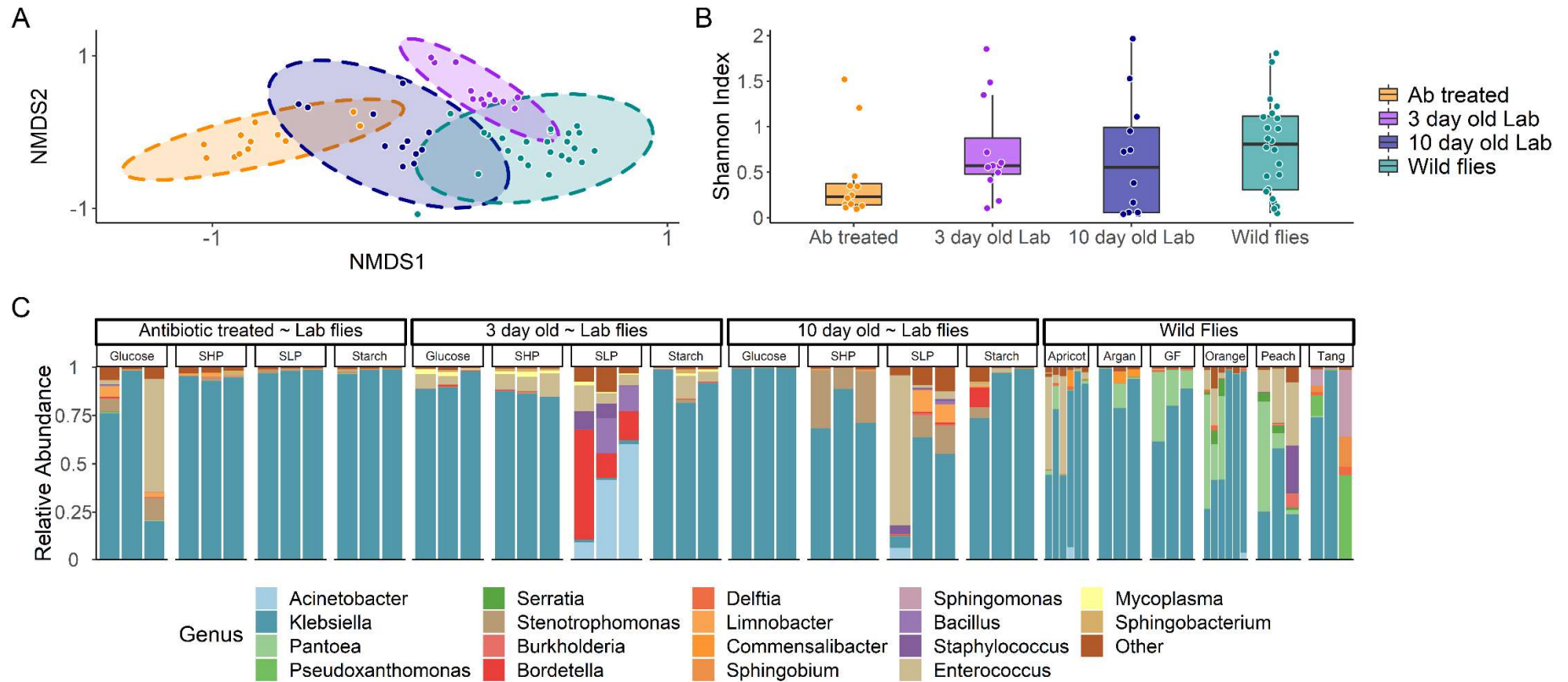
376

377 (i) *Bacterial community diversity*. We found that OTU richness and diversity varied significantly  
378 among host samples according to treatment and origin (Figure 1 A &B). Community structure (beta  
379 diversity) was affected primarily by diet, in both wild and lab flies (PERMANOVA:  $F_{8,48} = 2.74$ ,  $P$   
380  $<0.001$ ,  $R^2 = 0.27$ , Figure 1A). Within lab flies, age ( $F_{1,30} = 4.9$ ,  $P < 0.001$ ,  $R^2 = 0.18$ ), diet ( $F_{3,30} = 2.03$ ,  
381  $P = 0.023$ ,  $R^2 = 0.12$ ), and antibiotic treatment ( $F_{1,30} = 4.9$ ,  $P = 0.002$ ,  $R^2 = 0.09$ ), all affected  
382 community structure, with decreasing levels of effect. Bacterial species diversity (alpha diversity) did  
383 not vary significantly in the wild or laboratory population strains but was lower in antibiotic treated  
384 flies. However, the Shannon index was not significantly different between any samples (Figure 1B).  
385 Overall, we found no evidence of large-scale changes in diversity or composition of the microbiome  
386 despite testing multiple wild food sources, effects of laboratory diets and antibiotic treatment (Figure  
387 1C).

388

389 (ii) *Dominant bacterial taxa*. Four bacterial families representing two bacterial phyla made up over  
390 90% of the sequences in our dataset. These were the Proteobacteria, Enterobacteriaceae (79%),  
391 Moraxellaceae (2.3%) and Xanthomonadaceae (3.6%), and the Firmicutes, Enterococcus (7.3%)  
392 (Figure 1C). Of these, a single bacterial genus *Klebsiella* spp emerged as a core member of the  
393 bacterial microbiome. A putative *Klebsiella* spp was found in every medfly population sample and  
394 comprised 73.6% of the entire dataset. This suggests that, although medflies are extremely  
395 polyphagous, they have a stable microbiome, containing a recurrent *Klebsiella* spp symbiont.

396



397  
398  
399  
400  
401  
402  
403  
404

**Figure 1. 16S rRNA profiles of wild and laboratory strains of medfly on varied larval diets and in the presence and absence of antibiotic treatment.** Microbiome composition was measured as **(A)** community structure/beta diversity visualised as NMDS plots using a Bray-Curtis Dissimilarity Index with 95% confidence ellipses, **(B)** species richness/alpha diversity using the Shannon Index. Boxplot displays median, hinges are first and third quartiles, whiskers extend from hinge to 1.5\* the interquartile range. **(C)** Bar plot of microbiome profiles. Ab = antibiotic treated (100µg/ml kanamycin, 200 µg/ml ampicillin, 200 µg/ml streptomycin, 50 µg/ml chloramphenicol, 100µg/ml apramycin, 100 µg/ml hygromycin and 200 µg/ml tetracycline), 3 day old Lab = 3 day old adults from the Toliman laboratory strain; 10 day old Lab = 10 day old adults from the Toliman laboratory strain, wild flies = flies from fallen argan fruit in Arzou, Ait Melloul, Morocco; Apricots, Oranges and Grapefruits in Chania, Crete; and from Peaches, Oranges and Tangerines in Ano Lechonia, Greece (n = 5 flies per replicate, 3 biological replicates).

## 405 2. Medkleb genome sequencing

406 (i) *Classification of Medkleb sequencing contigs.* Total Medkleb DNA was sequenced on a PacBio  
407 RSII module and assembled using the HGAP.3 algorithm and Quiver (Chin et al., 2013). This  
408 process detected one large contig that sequestered 94% of total gene space (Figure 2) and four  
409 small contigs (mkp1-4; Figure S1). This suggests that the total Medkleb DNA complement is formed  
410 of one chromosome and four plasmids. Consistent with this, the mlplasmids software (Arredondo-  
411 Alonso et al., 2018) classified the large Medkleb contig as chromosomal and the four smaller contigs  
412 as plasmids (Table S2). In addition, mkp2, mkp3 and mkp4 were sequenced with relatively high  
413 coverage depth (Figure S2) and showed evidence for high copy numbers, a common plasmid trait  
414 (Providenti et al., 2006). Finally, mkp3 and mkp5 were demonstrated to have low GC content relative  
415 to the putative chromosome (Table S2), which again is characteristic of plasmid DNA (Nishida 2012).  
416 mkp2 and mkp4 both exhibited a similar GC content to that of the chromosome, suggesting that they  
417 have been acquired more recently (Rocha and Danchin 2002).

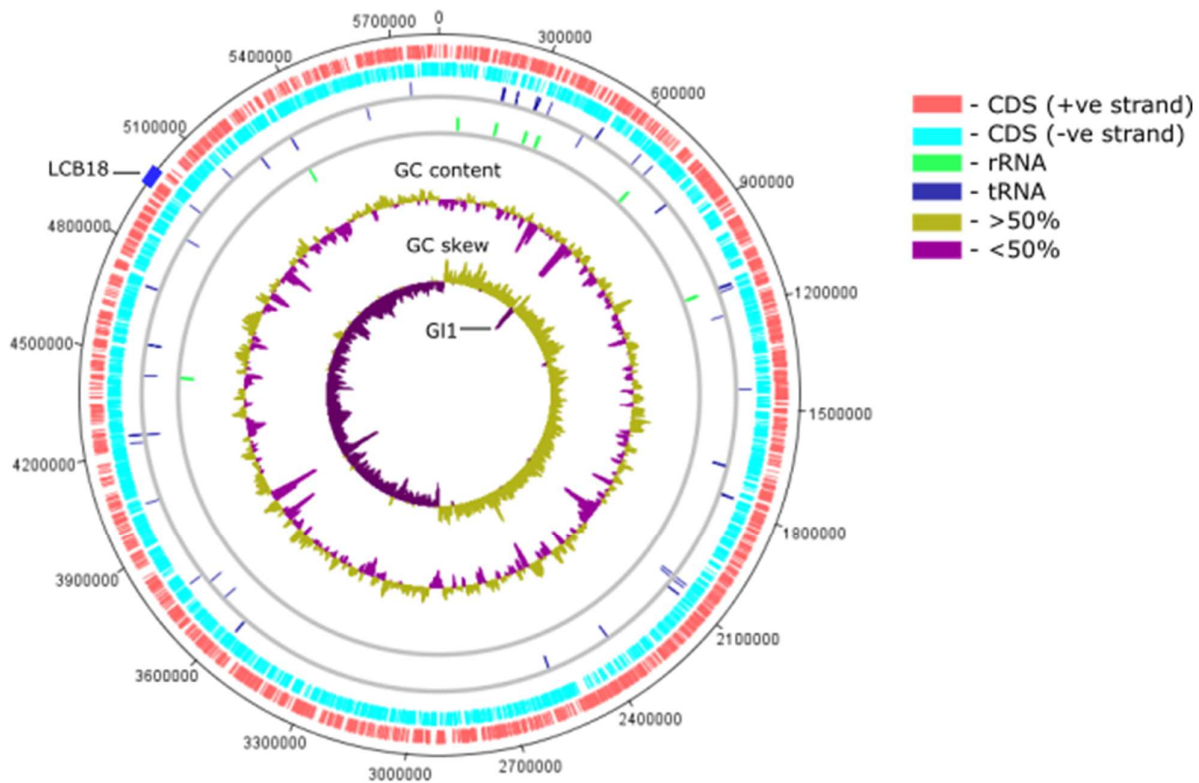
418 (ii) *Quality control.* PacBio coverage depth >100X is considered sufficient for resolving nucleotide  
419 sequences (Rhoads et al., 2015) and this threshold was met by all contigs other than mkp4 (Figure  
420 S2). The QV sequence resolution was 48.9 (an average error rate of 1 base in every 80100) and  
421 hence the Medkleb chromosome was of high quality (Figure S2). The plasmid QV's were: mkp1) 48,  
422 mkp2) 47.3, mkp3) 45.3 and mkp4) 44.8 (Figure S2). Although the plasmid sequences had lower  
423 resolution, they were robust, with accuracy >99.994% in all cases. The completeness of the Medkleb  
424 genome was measured with BUSCO (Simão et al 2015), which was used to search the assembly  
425 for 781 marker genes associated with bacteria of the *Enterobacteriales* order. BUSCO estimated  
426 that the Medkleb chromosomal sequence was 99.5% complete (777 of 781 genes complete and  
427 single copy), far exceeding general quality thresholds (Bowers et al 2017). Furthermore, three genes  
428 that were predicted by BUSCO to be fragmented were likely heterozygous alleles that failed to  
429 collapse during the annotation. CheckM (Parks et al 2015) was used as a second method to assess  
430 the Medkleb chromosome for completeness and contamination. By using as reference 1162 marker  
431 genes associated with the family *Enterobacteriaceae*, the CheckM software estimated that the  
432 Medkleb genome was 99.7% complete and 0.212% contaminated, again far exceeding standard  
433 quality thresholds (Bowers et al 2017).

434 (iii) *Medkleb genome.* The general characteristics of the Medkleb genome were consistent with those  
435 published as *Klebsiella oxytoca* (Shin et al 2012; Bao et al 2013). The Medkleb genome was 5 825  
436 435 nt in length, with 5 388 coding sequences and a GC content of 56.03% (Figure 2; Table S3). At  
437 87.8%, overall coding sequence was within the expected range (Kuo et al 2009), and, as predicted  
438 by Reva et al. (2004), genes were distributed symmetrically between the two DNA strands. There  
439 were 2 541 coding sequences on the positive strand, which were predicted to code for 2 473 proteins,  
440 50 tRNAs and 18 rRNAs. On the negative strand there were 2 847 coding sequences which coded  
441 for 2 805 proteins, 35 tRNAs and 7 rRNAs. KEGG (Kanehisa et al 2016) predicts that the Medkleb

442 genome encodes for genes with 2 842 distinct molecular functions. The genes for 16 (64%)  
443 ribosomal RNAs (rRNA) clustered between nts 62 435 – 70 701 near the origin of replication (*oriC*).  
444 Medkleb's GC content was 57.28% for protein coding genes, 53.83% for rRNA and 58.93% for tRNA.  
445 Consistent with Lobry (1996) GC skew was asymmetric, with an overrepresentation of Gs on the  
446 leading strand and Cs on the lagging strand, indicating that the genome is largely stable with few  
447 recent recombination events. However, there is one obvious exception, in which GC skew was  
448 inverted (>50% C's) between bases 654 265-677 695. This is indicative of a recent introgression  
449 that has resulted in the acquisition of a new gene island (designated G11) (Lawrence and Ochman  
450 1997; Wixon 2001).

451 (*iv*) *Medkleb* plasmids. The lengths and GC contents of mkps 1-4 (Table S2) were all within  
452 expected range for plasmids associated with *Klebsiella oxytoca*. mkps 1-4 are predicted by KEGG  
453 (Kanehisa et al 2016) to code for 48 functional orthologues and devote 14-22% of gene space to  
454 plasmid associated genes and mobile element coding sequences. This is substantial in comparison  
455 to the main chromosome, which only allocated 0.02% to such features. mkps 1, 3 and 4 exhibited  
456 asymmetric gene distribution between DNA strands (coding bias), which is common for plasmid  
457 genomes (Reva and Tümmler 2004). The coding bias of mkp3 was particularly clear, with ~90% of  
458 the total gene complement found on the positive strand. mkp4 was the only plasmid predicted by  
459 antiSMASH 6.0 beta (Blin et al 2019) to code for secondary metabolites, which included cloacin (de  
460 Graaf et al 1969) and colicin bacteriocins (Cascales et al 2007).

461



462

463 **Figure 2. Circular summary map of the Medkleb chromosome.** The Medkleb chromosome is represented  
464 with the stop codon (TGA) of the *dnaA* gene at position 0. Track one; 2 541 red ticks represent gene coding  
465 sequences on the positive strand. Track two; 2847 light blue ticks represent gene coding sequences on the  
466 negative strand. Track three; 50 dark blue ticks above the grey line represent tRNAs on the positive strand,  
467 and 35 ticks below the line represent tRNAs on the negative strand. Track four; 18 green ticks above the grey  
468 line represent rRNAs on the positive strand, and 7 ticks below the line represent rRNAs on the negative strand.  
469 64% of rRNAs are found close to *oriC*. Track five – GC content; regions containing >50% GC content are  
470 mustard and regions containing <50% GC content are purple. Track six – GC skew; regions containing >50%  
471 Gs are mustard and regions containing <50% Gs are purple. GC skew was asymmetric between leading and  
472 lagging strands, with the purple spike between bases 654 265-677 695 (G11) representing recent horizontal  
473 gene transfer (Lawrence and Ochman 1997). The LCB18 gene island ( $\approx$ nts  $4.97 \times 10^6 \sim 5 \times 10^6$ ) is represented  
474 by a blue block on the outer ring.

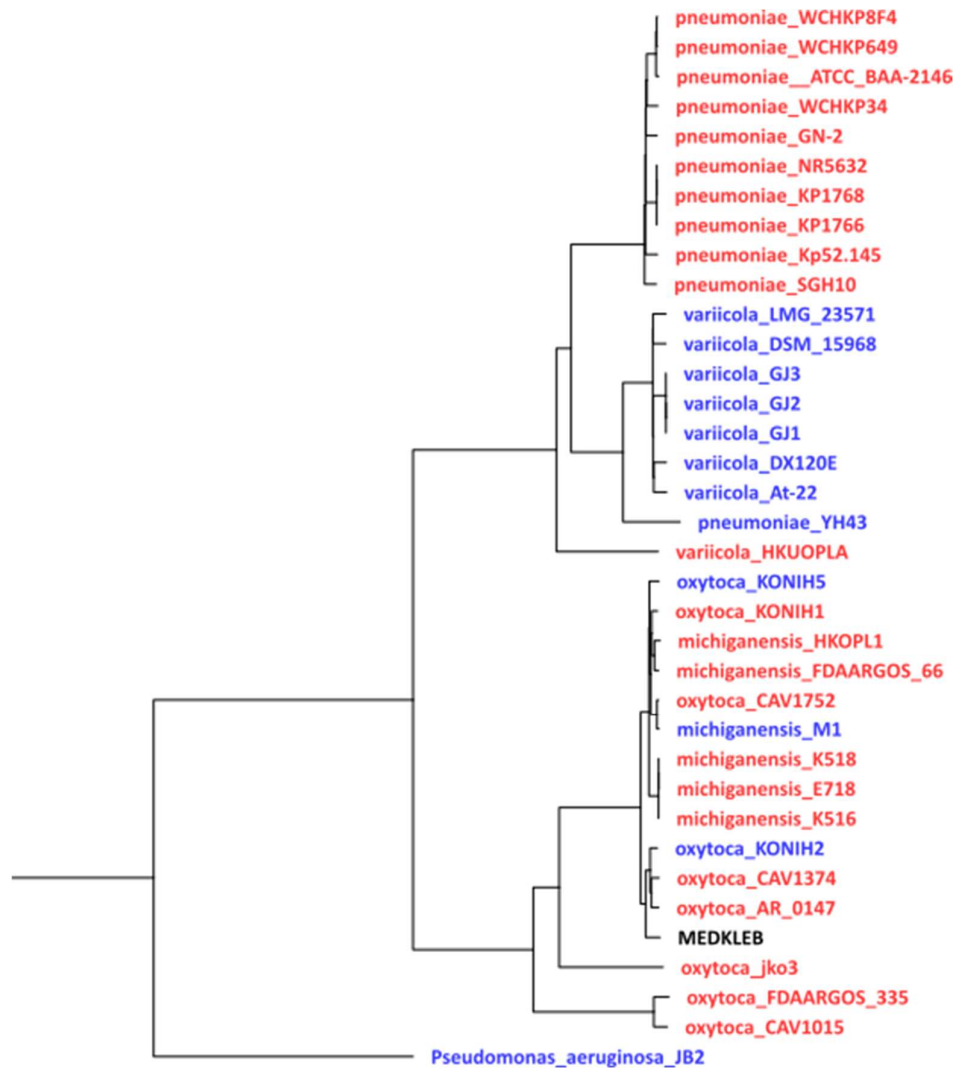
475



476 **3. Taxonomic placement of the Medkleb *Klebsiella* gut symbiont**

477 (i) *Taxonomic identification of Medkleb –16S rDNA and ANI analysis.* Medkleb was predicted to be  
478 a strain of *K. oxytoca*, which has previously been proposed as a major component of the medfly  
479 microbiome (Behar et al 2008a). The 16S rRNA gene sequence of *K. oxytoca* strain ATCC 13182  
480 (NR\_118853.1) was used to locate homologous sequences in the Medkleb genome using the  
481 BLASTn algorithm (Altschul et al 1997). This revealed that the Medkleb genome contains eight  
482 sequences >99% related to NR\_118853.1, which were all predicted to code for 16S rRNAs by  
483 RNAmmer 1.2 (Lagesen et al 2007). Nucleotides 341370-342821 (mk16S) which had the greatest  
484 homology with NR\_118853.1 were therefore used to represent Medkleb in subsequent taxonomic  
485 analyses. These sequences were used in an initial taxonomic description (as described in the  
486 Supplementary Information) which indicated that Medkleb was indeed likely to fall within a group of  
487 *Klebsiella oxytoca* / *michiganensis* spp (Figure S3).

488 A more stringent Average Nucleotide Identity (ANI) (Konstantinidis et al., 2005) analysis was also  
489 conducted. The Medkleb genome was positioned in an ANI matrix with 35 RefSeq *Klebsiella*  
490 genomes that were extracted from the NCBI database (Geer et al 2010) (Figure 3). This analysis  
491 placed Medkleb in a lineage with 13 strains classified as both *K. oxytoca* and *K. michiganensis*. ANI  
492 scores >95% are required to classify bacteria as the same species (Richter and Rosselló-Móra 2009;  
493 Kim et al 2014). This 95% similarity threshold was met by all thirteen members of Medkleb's ANI  
494 clade (henceforth referred to as the Medkleb group) (Figure S4). Hence both 16S rRNA gene and  
495 ANI analyses did not differentiate between *K. oxytoca* and *K. michiganensis* as they are currently  
496 named.



498 **Figure 3. ANI hierarchical clustering showing the evolutionary relationship of environmentally-derived**  
499 **and host-derived *Klebsiella* bacteria.** The tree was created using the ANI calculator (Figueras et al 2014),  
500 with *Pseudomonas aeruginosa* strain JB2 selected as the outgroup. Bacteria derived from animal hosts (red  
501 and black), and environmentally derived bacteria (blue), generally fell into three clades: 1) *K. pneumoniae*, 2)  
502 *K. variicola* and 3) *K. oxytoca/michiganensis*. With one exception in each group (YH43 and HKUOPLA), all *K.*  
503 *pneumoniae* are host derived and all *K. variicola* are environmentally derived. *K. oxytoca/K. michiganensis*  
504 have been isolated from both environmental and animal sources, but their sequences did not cluster according  
505 to source status. According to the ANI species threshold set by Kim et al. (2014), Medkleb is conspecific with  
506 twelve strains which have been classified as both *K. oxytoca* and *K. michiganensis*.

507

508 **4. Metabolic functions of the Medkleb *Klebsiella* gut symbiont**

509 (i) *Bioinformatic analyses of pectic lyases in Medkleb.* The ability to degrade pectin is a defining  
 510 phenotype of *K. oxytoca* and is proposed to be conferred by the polygalacturonase enzyme, *pehX*  
 511 (AY065648.1) (Kovtunovych et al 2003). We investigated whether *K. oxytoca* and *K. michiganensis*  
 512 strains of the Medkleb group could be distinguished via homology to *pehX* but our analysis detected  
 513 no significant differences between strains (analysed with BLAST; signed-rank linear model  $F_{1,11} =$   
 514 2.57,  $p = 0.137$ ). Unexpectedly, *K. michiganensis* shared greater homology with AY065648.1 than  
 515 did *K. oxytoca* (Table 1), despite the fact that *K. michiganensis* does not degrade pectin (Saha et al  
 516 2013). In addition, the CAZy database (Lombard et al 2010) identified two pectate lyases (one from  
 517 family 2 and one from family 9) in all Medkleb group genomes available on the database (Table S5).

518 **Table 1 Genomic features of the ‘Medkleb group’ of bacteria.** *pehX* sequence identity (calculated with  
 519 BLAST (Altschul et al., 1997)) was not significantly different between species (analysed with BLAST; signed-  
 520 rank linear model  $F_{1,11} = 2.57$ ,  $p = 0.137$ ). *K. michiganensis* genomes contained sequences more closely  
 521 related to AY065648.1 than was found for *K. oxytoca* genomes (mean relatedness = 88.4% vs 87.9%). All  
 522 genomes available on the CAZy database (Lombard et al 2010) are predicted to code for 2 pectate lyases.  
 523 Medkleb had the smallest genome in the group<sup>1</sup>, and the second highest GC content<sup>2</sup>.

Species	Strain	Genome size (nt)	GC (%)	<i>pehX</i> identity (%)	CAZy lyases
<i>oxytoca</i>	Medkleb	5825435 <sup>1</sup>	56.03	87.43	NA
<i>michiganensis</i>	M1	5865090	56.13 <sup>2</sup>	88.47	2
<i>michiganensis</i>	HKOPL1	5914407	55.92	88.56	2
<i>oxytoca</i>	CAV1752	5992008	55.16	88.47	2
<i>michiganensis</i>	FDAARGOS_66	6071464	55.94	88.39	NA
<i>michiganensis</i>	E718	6097032	56.02	88.31	2
<i>michiganensis</i>	K518	6138996	55.95	88.39	2
<i>michiganensis</i>	K516	6139574	55.96	88.31	2
<i>oxytoca</i>	KONIH1	6152190	55.91	88.61	2
<i>oxytoca</i>	KONIH5	6179177	55.81	87.82	2
<i>oxytoca</i>	KONIH2	6190364	55.77	87.43	2
<i>oxytoca</i>	CAV1374	6257473	55.75	87.87	2
<i>oxytoca</i>	AR_0147	6350620	55.57	87.89	2

<sup>1</sup> smallest genome

<sup>2</sup> highest GC content

524  
525

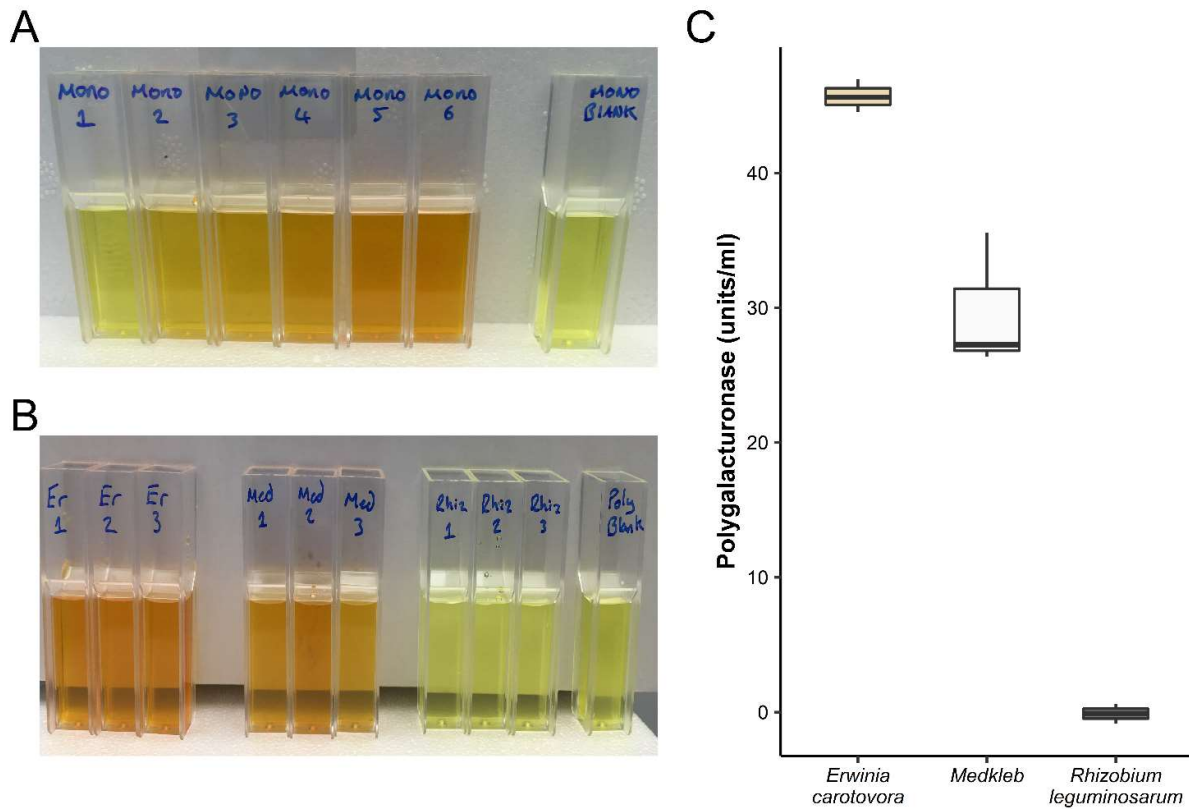
526 (ii) *Polygalacturonase enzyme assay.* Medkleb was *pehX* positive when analysed biochemically  
 527 (Figure S6), which suggested that it should be classified as *K. oxytoca* and can degrade pectin  
 528 (Kovtunovych et al 2003; Saha et al 2013). We quantified Medkleb’s capacity to degrade  
 529 polygalacturonic acid- in comparison to positive (*E carotovora*) and negative (*R leguminosarum*)  
 530 control specimens, using a DNS colorimetric method (Miller 1959). A standard curve of galacturonic  
 531 acid incubated with DNS (Figure 4A), showed a positive relationship with colour change when the

532 OD was measured at 530nm (linear model,  $F_{1,4} = 176.4$ ,  $p < 0.001$ ,  $R^2 = 0.97$ ). Filtrate of Medkleb  
533 and *E. carotovora* culture media both contained pectinolytic enzymes, producing measurable colour  
534 change when incubated with polygalacturonic acid and DNS (Figure 4B; (Sohail and Latif 2016)).  
535 Medkleb filtrate reduced polygalacturonic acid with around 65% the efficiency of the *Erwinia*  
536 *carotovora*, but *R leguminosarum* filtrate did not demonstrate any measurable pectinolytic activity  
537 (Figure 4C). These data support the placement of Medkleb as *K. oxytoca*.

538 (iii) *Predicted metabolic functions of Medkleb*. KEGG (Kanehisa et al 2016) was used to produce a  
539 list of gene functions for chromosomes and plasmids associated with all *K. oxytoca* bacteria in the  
540 Medkleb group (Table S5). The dataset was filtered to produce three smaller lists: 1) Atypical - gene  
541 functions unique to Medkleb, 2) Absent - gene functions present in all genomes analysed other  
542 than Medkleb, 3) Duplicated – gene functions encoded in multiple copies by Medkleb but not by any  
543 other genome analysed. The Medkleb genome contained 21 atypical functional orthologues (Figure  
544 S7), and of these, 16 were chromosomally derived and five located on plasmids. The atypical genes  
545 included two putative transposases, enzymes involved in various modes of metabolism (e.g., *mtlA*,  
546 *ACADSB*, *egsA*, *FAAH2*) and four transport protein genes (e.g. *natA* & *gatC*). When compared to  
547 conspecifics, Medkleb has 35 absent gene functions, seven of which may indicate adaptation to the  
548 relatively innocuous medfly gut (Figure S8). The largest cluster of absent genes was associated with  
549 copper resistance (*copB*, *cusS*, *cusR*, *cusC*, *cusF*) and genes that degrade arsenic (*arsB*) and nitriles  
550 (*nthA*) were also missing. The Medkleb genome codes for multiple copies of 11 functional  
551 orthologues, that other *K. oxytoca* bacteria in the Medkleb group retain in single copy at most (Figure  
552 S9). Medkleb's duplicated genes may have the potential to promote mutualistic phenotypes for the  
553 medfly, as they synthesise amino acids (*proC*, *trpA*) and metabolise beneficial nutrients such as fatty  
554 acids (*ACAT*) and citrate (*citE*).

555

556 (iv) *Secondary metabolites*. The Medkleb genome and plasmid sequences were interrogated using  
557 antiSMASH 6.0 beta (Blin et al 2019) for the presence of novel secondary metabolites.  
558 Chromosomes of all *K. oxytoca* members of the Medkleb group (other than KONIH2) coded for three  
559 common secondary metabolite clusters: 1) non-ribosomal polypeptide synthetase (30% similarity to  
560 turnerbactin), 2) thiopeptide antibiotic (14% similarity to O-antigen), 3) Ribosomally synthesized and  
561 post-translationally modified peptides (RiPPs). The Medkleb chromosome contained two unique  
562 secondary metabolite clusters that were not present in any other analysed *K. oxytoca* chromosomes  
563 (i) a butyrolactone, a signalling molecule utilised by *Streptomyces* bacteria to regulate antibiotic  
564 production and cell cycle processes (Takano 2006; Kitani et al 2011), and (ii) an N-acyl amino acid  
565 cluster, common to soil dwelling bacteria and involved in cell-to-cell communication (Craig et al 2011;  
566 Battista et al 2019) (Table 2). Plasmid mkp4 was also predicted to code for cloacin and colicin  
567 bacteriocins that were not coded by any other *K. oxytoca* strain in the Medkleb group. The cloacin  
568 cluster encoded on mkp4 contains two mobile elements (MKleb\_5887, MKleb\_5890) and is generally  
569 considered to be toxic for *Klebsiella* bacteria (de Graaf et al 1969).



570

571 **Figure 4. Polygalacturonase production by *Erwinia carotovora* (Er), Medkleb (Med) and *Rhizobium***  
572 ***leguminosarum* (Rhiz).** A) Monosaccharide colorimetric reaction mixtures, standard curve – The quantity of  
573 sugar in standards ranged from 0.9mg (mono 1) to 18mg (mono 6). Mono blank contained no sugar. When  
574 incubated with DNS, colour change (measured at  $\Delta A_{530}$ ) occurred for all reactions relative to the blank. The  
575 relationship between sugar quantity and colour change was significant (linear model,  $F_{1,4} = 176.4$ ,  $p < 0.001$ ,  
576  $R^2 = 0.98$ ). B) Bacteria reaction mixtures – Polygalacturonase production of three bacteria, *Erwinia carotovora*  
577 (Er), Medkleb (Med) and *Rhizobium leguminosarum* (Rhiz) was measured via the quantity of reduced sugar in  
578 solution, following incubation of culture filtrate with polygalacturonic acid. Units of polygalacturonase were  
579 quantified in terms of colour change via extrapolation from the standard curve. Med and Er filtrate contained  
580 30 and 46 units of polygalacturonase per ml respectively. Rhiz filtrate did not contain any polygalacturonase.  
581 C) Units of polygalacturonase contained in bacterial filtrate. Units of polygalacturonase per ml are represented  
582 on the y-axis. 1000ul aliquots of bacterial filtrate processed from three different species of bacteria are  
583 represented of the x-axis. Bacteria were assessed for the presence of polygalacturonases using a standard  
584 curve of galacturonic acid. The upper and lower hinges of boxplots represent the first and third quartiles of  
585 enzyme concentrations in filtrate, calculated from three technical replicates. *Erwinia carotovora* was the  
586 highest producer, with an average of 45.7 units/ml and Medkleb produced polygalacturonase with an average  
587 of 29.7 units/ml. *Rhizobium leguminosarum* did not produce any polygalacturonase.

588

## 589 **5. Searching for symbiotic signatures in the Medkleb genome**

590 (i) *Genome size and GC content.* At 5\_825\_435bp, the Medkleb genome was the smallest in the  
591 'Medkleb group' and 1.6 standard deviations smaller than the mean genome size of the clade (n=13)  
592 ( $\bar{x} = 6.07 \times 10^6$  bp  $\pm 1.49 \times 10^5$  s.d.). However, we conclude this is not diagnostic of symbiotic  
593 transition as the genome of free-living *K. michiganensis* strain M1, was only 0.7% larger than  
594 Medkleb ( $5.86 \times 10^6$  bp). Medkleb's GC content (56.03%) was also high, even for bacteria with a  
595 free-living life history (Moran et al 2008) (Table 1). We conclude that there were no obvious  
596 diagnostic signatures of a strong host-association.

597 (ii) *Local genomic rearrangement.* The Medkleb genome was aligned, using progressive Mauve  
598 (Darling et al 2010) to three closely related strains of *K. oxytoca* (Figure S5). This analysis revealed  
599 the presence of 21 local colinear blocks (LCBs) of conserved DNA in all four genomes (Figure S5).  
600 These LCBs were not uniformly distributed between the genomes. *K. oxytoca* strains AR0147 and  
601 CAV1374 both contained inversions between LCBs 11-16 and strain KONIH2 contained several  
602 instances of translocation and inversion. However, despite inversion and translocation events,  
603 nucleotide sequence in all LCBs other than LCB18 was very highly conserved. The annotation of  
604 Medkleb LCB18 ( $\approx$ nts  $4.97 \times 10^6 \sim 5 \times 10^6$ ) predicts 25 coding sequences in total, including 13  
605 "hypothetical proteins", 2 DNA helicases (Mkleb\_4576/4577), 2 methyltransferases  
606 (Mkleb\_4579/4597) and an anti-restriction protein (Mkleb\_4581). LCB18 may have been recently  
607 acquired as it also contains genes associated with horizontal transfer including an integrase  
608 (Mkleb\_4574), a mobile element protein (Mkleb\_4594) and a prophage protein (Mkleb\_4585). In  
609 addition, two hypothetical proteins encoded by LCB18 (Mkleb\_4591 & Mkleb\_4592) may be  
610 virulence factors, as they are predicted by TMHMM 2.0 (Krogh, 2001) to encode N-terminal peptides.  
611 However, there is as yet no definitive evidence that LCB18 contains genes that might confer fitness  
612 to the medfly (Table 2).

613

614 The Medkleb genome carries an inversion of GC skew on the leading strand (>50% C; region G11)  
615 indicating a putative horizontal gene transfer event. G11 is thought to have been transferred from a  
616 plasmid, as it codes for *TraY* which facilitates plasmid conjugal transfer (Nelson et al 1995). Though  
617 plasmid integration into host chromosome is common (Dobrindt et al 2004; Bire and Rouleux-Bonnin  
618 2012), G11 does not appear to have integrated from any of the Medkleb plasmids (mkps 1-4) (Table  
619 2). In total G11 is predicted to code for 25 proteins including BII0873, first sequenced in  
620 *Bradyrhizobium diazoefficiens*, a bacterium that is a known nitrogen fixing symbiont of legumes  
621 (Kaneko et al 2002). Interestingly, both G11 (Mkleb\_0586) and LCB18 (Mkleb\_4596) code for genes  
622 predicted to facilitate molybdopterin biosynthesis, which could have the potential to benefit the  
623 medfly host, as this group of co-factors aid nitrate reduction (Moreno-Vivián et al 1999).

624

625 According to KEGG analysis, the Medkleb genome contains coding sequences for 21 atypical  
626 functional orthologue genes that are not encoded in the genomes of any other closely related  
627 *Klebsiella* bacteria in the Medkleb group (Table 2). Some of these are potentially mutualistic  
628 functions such as sugar metabolism (*mtlA*) and nitrogen fixation (*nifZ*). Medkleb also has duplicates  
629 of 11 functional orthologues that *K. oxytoca* generally retains in only single copy. These duplicated  
630 functional orthologues do not cluster by genomic location. Several of these duplicated gene functions  
631 have strong mutualistic potential such as the biosynthesis of amino acids (*proC*, *trpA*) and  
632 breakdown of essential nutrients (*cite*, *pydC*). In contrast, Medkleb is also missing some clusters of  
633 genes that are present in closely related bacteria, e.g. for specific enzymes related to copper  
634 resistance (*copB*, *cusS*, *cusR*, *cusC*, *cusF*) and phosphonate transport (*phnC*, *phnD*, *phnE*).

635 **Table 2 Unique features of the Medkleb genome in comparison to conspecifics.**

Unique feature	Identified via	Possible mutualistic function
<i>LCB18</i>	progressiveMauve analysis of Medkleb and three conspecifics	Codes for genes related to molybdopterin biosynthesis and several proteins with unknown function. These genes may confer fitness to the medfly.
<i>G11</i>	Inversion of GC skew	Codes for genes related to molybdopterin biosynthesis and several proteins with unknown function. These genes may confer fitness to the medfly.
<i>Atypical metabolic genes</i>	Comparison of KEGG gene functions between Medkleb group members.	<i>mtlA</i> , <i>ACADSB</i> , <i>egsA</i> and <i>FAAH2</i> expand the range of nutrients available to the medfly.
<i>Absent sensory genes</i>	Comparison of KEGG gene functions between Medkleb group members.	The medfly gut may be relatively non-toxic allowing Medkleb to survive without genes that detect and metabolise certain chemical threats in its environment ( <i>copB</i> , <i>cusS</i> , <i>cusR</i> , <i>cusC</i> , <i>cusF</i> , <i>arsB</i> , <i>nthA</i> ).
<i>Duplicated genes</i>	Comparison of KEGG gene functions between Medkleb group members	Duplication of 11 genes associated with biosynthesis of amino acids and breakdown of essential nutrients. These genes may confer fitness to the medfly by providing access to extra nutritional resources

Unique feature	Identified via	Possible mutualistic function
<i>Butyrolactone biosynthesis</i>	antiSMASH 6.0 beta	Possible regulation of antibiotic products (Takano 2006; Kitani et al 2011)
<i>N-acyl amino acid biosynthesis</i>	antiSMASH 6.0 beta	An important family of endogenous signalling molecules in which an amide bond covalently links an amino acid to the acyl moiety of a long-chain fatty acid. Primarily involved in cell-to-cell communication (Craig et al 2011; Battista et al 2019_

636

## 637 Discussion

638

### 639 The medfly microbiome

640 In this study, we report the use of laboratory and field-reared adult medflies to characterise key  
641 features of the bacterial microbiome of this important agricultural pest. Using analyses of 16S rRNA  
642 gene amplicon sequencing of culturable and non-culturable members of the gut microbiome, we  
643 found that overall species richness was fairly stable between the laboratory-reared flies raised on  
644 different diets and the wild medfly samples. Direct comparisons of beta diversity indicated that larval  
645 diet, rather than exposure to antibiotics or wild vs lab rearing was the primary driver of microbial  
646 diversity of gut microbiomes. Wild flies obtained from distinct geographical regions and different  
647 hosts and flies reared on different substrates and exposed to antibiotic cocktails in the laboratory,  
648 contained largely the same bacterial families. The data suggest that although medflies are highly  
649 polyphagous, they have a stable microbiome that is dominated by the bacterial family  
650 *Enterobacteriaceae*, including a putative symbiont *Klebsiella* spp. These findings are consistent with  
651 previous analyses of medfly microbiomes made using culture-based methods (Behar et al 2005;  
652 Behar et al 2008a; Behar et al 2008b; Behar et al 2009a). The picture may be more complex,  
653 however, as one recent next-generation sequencing study did not isolate *Klebsiella* in medfly  
654 microbiomes from wild populations (Malacrino et al 2018), and another identified possible  
655 geographic or host-genetic structure links with bacterial dominance (with samples from Greece being  
656 dominated by *Klebsiella* spp) (Nikolouli et al 2020).

657

### 658 Genome sequencing and analysis of the putative Medkleb gut symbiont

659 We obtained a fully sequenced Medkleb genome and both 16S rRNA gene and ANI phylogenies  
660 identified this as a *Klebsiella* species (Stackebrandt 2006; Kim et al 2014). Medkleb was *pehX*  
661 positive when analysed with PCR, and a producer of pectinolytic enzymes, both of which support its  
662 identification as *K. oxytoca* (Kovtunovych et al 2003; Saha et al 2013).

663



664 Genome size and GC content are generally reduced when a bacterium adopts a facultative lifestyle  
665 (McCutcheon and Moran 2011). We found that, although the Medkleb genome was the smallest of  
666 all *Klebsiella* bacteria in the 'Medkleb group', the free-living *K. michiganensis* strain M1 was only 40  
667 kb (0.7%) larger. The Medkleb GC content was also the second highest in the 'Medkleb group', again  
668 counter to what is expected for a facultative mutualist. A strongly symbiotic transition is generally  
669 associated with an increased mutation rate, which causes facultative symbionts to occupy extended  
670 branches of phylogenetic trees (McCutcheon and Moran 2011). Though Medkleb was slightly distinct  
671 from the three bacterial species most closely related to it, it was not markedly so.

672

673 We also used high resolution comparative genetic techniques to test for signals of putative  
674 mutualism. These analyses were designed to test: (i) If Medkleb possessed genetic loci/functions  
675 that were absent from closely related *Klebsiella* bacteria and possessed an obvious mutualistic  
676 capacity for the fly; (ii) If Medkleb was lacking genetic loci/functions found in all closely related free-  
677 living *Klebsiella* spp., that would be considered necessary for life in varied environments. Set against  
678 this is that gene loss may be unpredictable in the early stages of facultative mutualistic transitions  
679 (Moran and Bennett 2014).

680

681 Comparative genomics highlighted that the Medkleb genome contained two discrete regions (GI1  
682 and LCB18) which may have been acquired comparatively recently and are not typically found in *K.*  
683 *oxytoca*. Both GI1 and LCB18 contain genes associated with horizontal transfer and encode several  
684 unannotated hypothetical proteins with mutualistic potential. Medkleb was demonstrated to be  
685 functionally pectinolytic and global gene function analyses highlighted several more atypical  
686 functions were encoded exclusively by Medkleb in comparison to conspecifics. These atypical genes  
687 are dispersed throughout the genome which suggests that they are ancestral and not recently  
688 inherited. Some of these genes are predicted to encode metabolic enzymes that could allow the  
689 medfly to utilise otherwise unattainable nutrients. In addition, Medkleb has several duplicated genes  
690 that are randomly distributed throughout the genome which could provide the medfly with beneficial  
691 nutrients and amino acids. Together, these genomic signatures suggest that Medkleb is a symbiont  
692 that improves host fitness through increased access to vital nutrients. If substantiated, this could  
693 help to partially explain the success of the medfly as a generalist pest. However, potentially  
694 mutualistic traits are not evidence of mutualism itself and many signals that are commonly associated  
695 with facultative mutualism are not evident in the Medkleb genome. Therefore there is insufficient  
696 evidence, so far, to definitively classify Medkleb as a facultative mutualist of the medfly.

697

698 *Klebsiella* bacteria and the medfly appear to co-occur almost universally (Behar et al 2009b; Leftwich  
699 2012). Therefore, Medkleb might provide a platform for paratransgenic control of the medfly. This  
700 study is one of only a handful of comprehensive characterisations of the bacterial symbionts of the  
701 tephritid fruit fly *C. capitata* using culture-independent methods, and the first to characterise the

702 genome of a putative symbiont. Future studies should sample all developmental stages of the  
703 medfly, and sample more intensively to establish the potential for phyllosymbiosis. Complementing  
704 this should be experimental studies to establish localisation of *Klebsiella* within the medfly gut, to  
705 determine transmission mechanisms and assess metabolic communication and host benefit  
706 (Leftwich et al 2020).

707

708 **Data Deposition:**

709 Sequencing data has been submitted to the NCBI Sequence Read Archive and is available under  
710 BioProject ID PRJNA638617.

711

712 **Acknowledgements**

713 This work was funded by the Biotechnology and Biological Sciences Research Council Research  
714 (Grant BB/K000489/1 to T.C., P.T.L., and M.I.H. and PhD studentship to M.D). We also thank  
715 Kostas Voudouris, Romisa Asadi & Martha Koukidou for their help in collecting samples for  
716 analysis.

717

## 718 References

- 719 Aharon Y, Pasternak Z, Ben Yosef M, et al (2013) Phylogenetic, metabolic, and taxonomic  
720 diversities shape Mediterranean fruit fly microbiotas during ontogeny. *Appl Environ*  
721 *Microbiol* 79:303–313. doi: 10.1128/AEM.02761-12
- 722 Altschul SF, Madden TL, Schäffer AA, et al (1997) Gapped BLAST and PSI-BLAST: a new  
723 generation of protein database search programs. *Nucleic Acids Res* 25:3389–3402. doi:  
724 10.1093/nar/25.17.3389
- 725 Anbutsu H, Moriyama M, Nikoh N, et al (2017) Small genome symbiont underlies cuticle hardness  
726 in beetles. *Proc Natl Acad Sci USA* 114:E8382–E8391. doi: 10.1073/pnas.1712857114
- 727 Arredondo-Alonso S, Rogers MRC, Braat JC, et al (2018) miplasmids: a user-friendly tool to  
728 predict plasmid- and chromosome-derived sequences for single species. *Microb Genom.*  
729 doi: 10.1099/mgen.0.000224
- 730 Ballinger MJ, Perlman SJ (2017) Generality of toxins in defensive symbiosis: Ribosome-  
731 inactivating proteins and defense against parasitic wasps in *Drosophila*. *PLoS Pathog*  
732 13:e1006431. doi: 10.1371/journal.ppat.1006431
- 733 Bao G, Zhang Y, Du C, et al (2013) Genome Sequence of *Klebsiella oxytoca* M5a1, a Promising  
734 Strain for Nitrogen Fixation and Chemical Production. *Genome Announc.* doi:  
735 10.1128/genomeA.00074-12
- 736 Battista N, Bari M, Bisogno T (2019) N-Acyl Amino Acids: Metabolism, Molecular Targets, and  
737 Role in Biological Processes. *Biomolecules.* doi: 10.3390/biom9120822
- 738 Behar A, Ben-Yosef M, Lauzon CR, et al (2009a) Structure and function of the bacterial community  
739 associated with the Mediterranean fruit fly. *Insect Symbiosis*
- 740 Behar A, Ben-Yosef M, Lauzon CR, et al (2009b) Structure and function of the bacterial community  
741 associated with the Mediterranean fruit fly. 251–271.
- 742 Behar A, Jurkevitch E, Yuval B (2008a) Bringing back the fruit into fruit fly-bacteria interactions.  
743 *Mol Ecol* 17:1375–1386. doi: 10.1111/j.1365-294X.2008.03674.x
- 744 Behar A, Yuval B, Jurkevitch E (2008b) Gut bacterial communities in the Mediterranean fruit fly  
745 (*Ceratitis capitata*) and their impact on host longevity. *J Insect Physiol* 54:1377–1383. doi:  
746 10.1016/j.jinsphys.2008.07.011
- 747 Behar A, Yuval B, Jurkevitch E (2005) Enterobacteria-mediated nitrogen fixation in natural  
748 populations of the fruit fly *Ceratitis capitata*. *Mol Ecol* 14:2637–2643. doi: 10.1111/j.1365-  
749 294X.2005.02615.x
- 750 Ben Ami E, Yuval B, Jurkevitch E (2010) Manipulation of the microbiota of mass-reared  
751 Mediterranean fruit flies *Ceratitis capitata* (Diptera: Tephritidae) improves sterile male  
752 sexual performance. *ISME J* 4:28–37. doi: 10.1038/ismej.2009.82
- 753 Ben-Yosef M, Pasternak Z, Jurkevitch E, Yuval B (2014) Symbiotic bacteria enable olive flies  
754 (*Bactrocera oleae*) to exploit intractable sources of nitrogen. *J Evol Biol* 27:2695–2705. doi:  
755 10.1111/jeb.12527
- 756 Bennett GM, Moran NA (2013) Small, smaller, smallest: the origins and evolution of ancient dual  
757 symbioses in a Phloem-feeding insect. *Genome Biol Evol* 5:1675–1688. doi:  
758 10.1093/gbe/evt118
- 759 Bire S, Rouleux-Bonnin F (2012) Transposable elements as tools for reshaping the genome: it is a  
760 huge world after all! *Methods Mol Biol* 859:1–28. doi: 10.1007/978-1-61779-603-6\_1
- 761 Blin K, Shaw S, Steinke K, et al (2019) antiSMASH 5.0: updates to the secondary metabolite  
762 genome mining pipeline. *Nucleic Acids Res* 47:W81–W87. doi: 10.1093/nar/gkz310
- 763 Bosco-Drayon V, Poidevin M, Boneca IG, et al (2012) Peptidoglycan sensing by the receptor  
764 PGRP-LE in the *Drosophila* gut induces immune responses to infectious bacteria and  
765 tolerance to microbiota. *Cell Host Microbe* 12:153–165. doi: 10.1016/j.chom.2012.06.002
- 766 Bowers RM, Kyrpides NC, Stepanauskas R, et al (2017) Minimum information about a single  
767 amplified genome (MISAG) and a metagenome-assembled genome (MIMAG) of bacteria  
768 and archaea. *Nat Biotechnol* 35:725–731. doi: 10.1038/nbt.3893
- 769 Carver T, Thomson N, Bleasby A, et al (2009) DNAPlotter: circular and linear interactive genome  
770 visualization. *Bioinformatics* 25:119–120. doi: 10.1093/bioinformatics/btn578
- 771 Cascales E, Buchanan SK, Duché D, et al (2007) Colicin biology. *Microbiol Mol Biol Rev* 71:158–  
772 229. doi: 10.1128/MMBR.00036-06

- 773 Chandler JA, Lang JM, Bhatnagar S, et al (2011) Bacterial communities of diverse *Drosophila*  
774 species: ecological context of a host-microbe model system. *PLoS Genet* 7:e1002272. doi:  
775 10.1371/journal.pgen.1002272
- 776 Chin C-S, Alexander DH, Marks P, et al (2013) Nonhybrid, finished microbial genome assemblies  
777 from long-read SMRT sequencing data. *Nat Methods* 10:563–569. doi:  
778 10.1038/nmeth.2474
- 779 Craig JW, Cherry MA, Brady SF (2011) Long-chain N-acyl amino acid synthases are linked to the  
780 putative PEP-CTERM/exosortase protein-sorting system in Gram-negative bacteria. *J*  
781 *Bacteriol* 193:5707–5715. doi: 10.1128/JB.05426-11
- 782 Darling AE, Mau B, Perna NT (2010) progressiveMauve: multiple genome alignment with gene  
783 gain, loss and rearrangement. *PLoS One* 5:e11147. doi: 10.1371/journal.pone.0011147
- 784 de Graaf FK, Spanjaerdts Speckman EA, Stouthamer AH (1969) Mode of action of a bacteriocin  
785 produced by *Enterobacter cloacae* DF13. *Antonie Van Leeuwenhoek* 35:287–306.
- 786 de Souza DJ, Bézier A, Depoix D, et al (2009) *Blochmannia* endosymbionts improve colony growth  
787 and immune defence in the ant *Camponotus fellah*. *BMC Microbiol* 9:29. doi:  
788 10.1186/1471-2180-9-29
- 789 Deguenon JM, Travanty N, Zhu J, et al (2019) Exogenous and endogenous microbiomes of wild-  
790 caught *Phormia regina* (Diptera: Calliphoridae) flies from a suburban farm by 16S rRNA  
791 gene sequencing. *Sci Rep* 9:20365. doi: 10.1038/s41598-019-56733-z
- 792 Dobrindt U, Hochhut B, Hentschel U, Hacker J (2004) Genomic islands in pathogenic and  
793 environmental microorganisms. *Nat Rev Microbiol* 2:414–424. doi: 10.1038/nrmicro884
- 794 Durvasula RV, Gumbs A, Panackal A, et al (1997) Prevention of insect-borne disease: an  
795 approach using transgenic symbiotic bacteria. *Proc Natl Acad Sci USA* 94:3274–3278. doi:  
796 10.1073/pnas.94.7.3274
- 797 Figueras MJ, Beaz-Hidalgo R, Hossain MJ, Liles MR (2014) Taxonomic affiliation of new genomes  
798 should be verified using average nucleotide identity and multilocus phylogenetic analysis.  
799 *Genome Announc*. doi: 10.1128/genomeA.00927-14
- 800 Gascuel O (1997) BIONJ: an improved version of the NJ algorithm based on a simple model of  
801 sequence data. *Mol Biol Evol* 14:685–695. doi: 10.1093/oxfordjournals.molbev.a025808
- 802 Gavriel S, Jurkevitch E, Gazit Y, Yuval B (2011) Bacterially enriched diet improves sexual  
803 performance of sterile male Mediterranean fruit flies. *J Appl Entomology* 135:564–573. doi:  
804 10.1111/j.1439-0418.2010.01605.x
- 805 Geer LY, Marchler-Bauer A, Geer RC, et al (2010) The NCBI BioSystems database. *Nucleic Acids*  
806 *Res* 38:D492–6. doi: 10.1093/nar/gkp858
- 807 Gould AL, Zhang V, Lamberti L, et al (2018) Microbiome interactions shape host fitness. *Proc Natl*  
808 *Acad Sci USA* 115:E11951–E11960. doi: 10.1073/pnas.1809349115
- 809 Hansen TB, Wiklund ED, Bramsen JB, et al (2011) miRNA-dependent gene silencing involving  
810 Ago2-mediated cleavage of a circular antisense RNA. *EMBO J* 30:4414–4422. doi:  
811 10.1038/emboj.2011.359
- 812 Heine D, Holmes NA, Worsley SF, et al (2018) Chemical warfare between leafcutter ant symbionts  
813 and a co-evolved pathogen. *Nat Commun* 9:2208. doi: 10.1038/s41467-018-04520-1
- 814 Holmes NA, Innocent TM, Heine D, et al (2016) Genome analysis of two  
815 *Pseudonocardia* phylotypes associated with *Acromyrmex* leafcutter ants reveals their  
816 biosynthetic potential. *Front Microbiol* 7:2073. doi: 10.3389/fmicb.2016.02073
- 817 Hurst GDD, Frost CL (2015) Reproductive parasitism: maternally inherited symbionts in a  
818 biparental world. *Cold Spring Harb Perspect Biol*. doi: 10.1101/cshperspect.a017699
- 819 Husnik F, Nikoh N, Koga R, et al (2013) Horizontal gene transfer from diverse bacteria to an insect  
820 genome enables a tripartite nested mealybug symbiosis. *Cell* 153:1567–1578. doi:  
821 10.1016/j.cell.2013.05.040
- 822 Hyatt D, Chen G-L, Locascio PF, et al (2010) Prodigal: prokaryotic gene recognition and  
823 translation initiation site identification. *BMC Bioinformatics* 11:119. doi: 10.1186/1471-2105-  
824 11-119
- 825 Jurkevitch E (2011) Riding the Trojan horse: combating pest insects with their own symbionts.  
826 *Microb Biotechnol* 4:620–627. doi: 10.1111/j.1751-7915.2011.00249.x
- 827 Kanehisa M, Sato Y, Kawashima M, et al (2016) KEGG as a reference resource for gene and  
828 protein annotation. *Nucleic Acids Res* 44:D457–62. doi: 10.1093/nar/gkv1070

- 829 Kaneko T, Nakamura Y, Sato S, et al (2002) Complete genomic sequence of nitrogen-fixing  
830 symbiotic bacterium *Bradyrhizobium japonicum* USDA110 (supplement). DNA Res 9:225–  
831 256. doi: 10.1093/dnares/9.6.225
- 832 Kim M, Oh H-S, Park S-C, Chun J (2014) Towards a taxonomic coherence between average  
833 nucleotide identity and 16S rRNA gene sequence similarity for species demarcation of  
834 prokaryotes. Int J Syst Evol Microbiol 64:346–351. doi: 10.1099/ij.s.0.059774-0
- 835 Kitani S, Miyamoto KT, Takamatsu S, et al (2011) Avenolide, a Streptomyces hormone controlling  
836 antibiotic production in *Streptomyces avermitilis*. Proc Natl Acad Sci USA 108:16410–  
837 16415. doi: 10.1073/pnas.1113908108
- 838 Konstantinidis KT, Tiedje JM (2005) Genomic insights that advance the species definition for  
839 prokaryotes. Proc Natl Acad Sci USA 102:2567–2572. doi: 10.1073/pnas.0409727102
- 840 Kovtunovych G, Lytvynenko T, Negrutskaya V, et al (2003) Identification of *Klebsiella oxytoca* using a  
841 specific PCR assay targeting the polygalacturonase *pehX* gene. Res Microbiol 154:587–  
842 592. doi: 10.1016/S0923-2508(03)00148-7
- 843 Kuo C-H, Moran NA, Ochman H (2009) The consequences of genetic drift for bacterial genome  
844 complexity. Genome Res 19:1450–1454. doi: 10.1101/gr.091785.109
- 845 Lagesen K, Hallin P, Rødland EA, et al (2007) RNAmmer: consistent and rapid annotation of  
846 ribosomal RNA genes. Nucleic Acids Res 35:3100–3108. doi: 10.1093/nar/gkm160
- 847 Lauzon CR, McCombs SD, Potter SE, Peabody NC (2009) Establishment and vertical passage of  
848 Enterobacter (*Pantoea*) agglomerans and *Klebsiella pneumoniae* through all life stages of  
849 the Mediterranean fruit fly (Diptera: Tephritidae). Ann Entomol Soc Am 102:85–95.
- 850 Lawrence JG, Ochman H (1997) Amelioration of bacterial genomes: rates of change and  
851 exchange. J Mol Evol 44:383–397. doi: 10.1007/pl00006158
- 852 Lee C, Grasso C, Sharlow MF (2002) Multiple sequence alignment using partial order graphs.  
853 Bioinformatics 18:452–464. doi: 10.1093/bioinformatics/18.3.452
- 854 Leftwich PT (2012) Male reproductive success and population control in the Mediterranean fruit fly,  
855 *Ceratitis capitata*. Doctoral Thesis, University of East Anglia
- 856 Leftwich PT, Bolton M, Chapman T (2016) Evolutionary biology and genetic techniques for insect  
857 control. Evol Appl 9:212–230. doi: 10.1111/eva.12280
- 858 Leftwich PT, Clarke NVE, Hutchings MI, Chapman T (2018) Reply to Obadia et al.: Effect of methyl  
859 paraben on host-microbiota interactions in *Drosophila melanogaster*. Proc Natl Acad Sci  
860 USA 115:E4549–E4550. doi: 10.1073/pnas.1805499115
- 861 Leftwich PT, Edgington MP, Chapman T (2020) Transmission efficiency drives host-microbe  
862 associations. Proc Biol Sci 287:20200820. doi: 10.1098/rspb.2020.0820
- 863 Leftwich PT, Nash WJ, Friend LA, Chapman T (2017) Adaptation to divergent larval diets in the  
864 medfly, *Ceratitis capitata*. Evolution 71:289–303. doi: 10.1111/evo.13113
- 865 Lhocine N, Ribeiro PS, Buchon N, et al (2008) PIMS modulates immune tolerance by negatively  
866 regulating *Drosophila* innate immune signaling. Cell Host Microbe 4:147–158. doi:  
867 10.1016/j.chom.2008.07.004
- 868 Lindberg BG, Tang X, Dantoft W, et al (2018) Nubbin isoform antagonism governs *Drosophila*  
869 intestinal immune homeostasis. PLoS Pathog 14:e1006936. doi:  
870 10.1371/journal.ppat.1006936
- 871 Liu LJ, Martínez-Sañudo I, Mazzon L, et al (2016) Bacterial communities associated with invasive  
872 populations of *Bactrocera dorsalis* (Diptera: Tephritidae) in China. Bull Entomol Res  
873 106:718–728. doi: 10.1017/S0007485316000390
- 874 Lobry JR (1996) Asymmetric substitution patterns in the two DNA strands of bacteria. Mol Biol Evol  
875 13:660–665. doi: 10.1093/oxfordjournals.molbev.a025626
- 876 Lombard V, Bernard T, Rancurel C, et al (2010) A hierarchical classification of polysaccharide  
877 lyases for glycogenomics. Biochem J 432:437–444. doi: 10.1042/BJ20101185
- 878 Malacrinò A, Campolo O, Medina RF, Palmeri V (2018) Instar- and host-associated differentiation  
879 of bacterial communities in the Mediterranean fruit fly *Ceratitis capitata*. PLoS One  
880 13:e0194131. doi: 10.1371/journal.pone.0194131
- 881 McCutcheon JP, Moran NA (2011) Extreme genome reduction in symbiotic bacteria. Nat Rev  
882 Microbiol 10:13–26. doi: 10.1038/nrmicro2670
- 883 McFall-Ngai M, Hadfield MG, Bosch TCG, et al (2013) Animals in a bacterial world, a new  
884 imperative for the life sciences. Proc Natl Acad Sci USA 110:3229–3236. doi:  
885 10.1073/pnas.1218525110

- 886 McMurdie PJ, Holmes S (2013) phyloseq: an R package for reproducible interactive analysis and  
887 graphics of microbiome census data. PLoS One 8:e61217. doi:  
888 10.1371/journal.pone.0061217
- 889 Miller GL (1959) Use of dinitrosalicylic acid reagent for determination of reducing sugar. Anal  
890 Chem 31:426–428. doi: 10.1021/ac60147a030
- 891 Moran NA, Bennett GM (2014) The tiniest tiny genomes. Annu Rev Microbiol 68:195–215. doi:  
892 10.1146/annurev-micro-091213-112901
- 893 Moran NA, McCutcheon JP, Nakabachi A (2008) Genomics and evolution of heritable bacterial  
894 symbionts. Annu Rev Genet 42:165–190. doi: 10.1146/annurev.genet.41.110306.130119
- 895 Moran NA, Tran P, Gerardo NM (2005) Symbiosis and insect diversification: an ancient symbiont  
896 of sap-feeding insects from the bacterial phylum Bacteroidetes. Appl Environ Microbiol  
897 71:8802–8810. doi: 10.1128/AEM.71.12.8802-8810.2005
- 898 Moreno-Vivián C, Cabello P, Martínez-Luque M, et al (1999) Prokaryotic nitrate reduction:  
899 molecular properties and functional distinction among bacterial nitrate reductases. J  
900 Bacteriol 181:6573–6584. doi: 10.1128/JB.181.21.6573-6584.1999
- 901 Negri I, Franchini A, Gonella E, et al (2009) Unravelling the Wolbachia evolutionary role: the  
902 reprogramming of the host genomic imprinting. Proc Biol Sci 276:2485–2491. doi:  
903 10.1098/rspb.2009.0324
- 904 Nelson WC, Howard MT, Sherman JA, Matson SW (1995) The *traY* gene product and integration  
905 host factor stimulate *Escherichia coli* DNA helicase I-catalyzed nicking at the F plasmid  
906 oriT. J Biol Chem 270:28374–28380.
- 907 Nikolouli K, Augustinos AA, Stathopoulou P, et al (2020) Genetic structure and symbiotic profile of  
908 worldwide natural populations of the Mediterranean fruit fly, *Ceratitidis capitata*. BMC Genet  
909 21:128. doi: 10.1186/s12863-020-00946-z
- 910 Nishida H (2012) Comparative analyses of base compositions, DNA sizes, and dinucleotide  
911 frequency profiles in archaeal and bacterial chromosomes and plasmids. Int J Evol Biol  
912 2012:342482. doi: 10.1155/2012/342482
- 913 Ochman H, Davalos LM (2006) The nature and dynamics of bacterial genomes. Science  
914 311:1730–1733. doi: 10.1126/science.1119966
- 915 Ochman H, Lawrence JG, Groisman EA (2000) Lateral gene transfer and the nature of bacterial  
916 innovation. Nature 405:299–304. doi: 10.1038/35012500
- 917 Oksanen J, Kindt R, Legendre P, O'Hara B (2007) The vegan package. Community ecology ...
- 918 Oliver KM, Russell JA, Moran NA, Hunter MS (2003) Facultative bacterial symbionts in aphids  
919 confer resistance to parasitic wasps. Proc Natl Acad Sci USA 100:1803–1807. doi:  
920 10.1073/pnas.0335320100
- 921 Overbeek R, Olson R, Pusch GD, et al (2014) The SEED and the Rapid Annotation of microbial  
922 genomes using Subsystems Technology (RAST). Nucleic Acids Res 42:D206–14. doi:  
923 10.1093/nar/gkt1226
- 924 Parks DH, Imelfort M, Skennerton CT, et al (2015) CheckM: assessing the quality of microbial  
925 genomes recovered from isolates, single cells, and metagenomes. Genome Res 25:1043–  
926 1055. doi: 10.1101/gr.186072.114
- 927 Peplies J, Kottmann R, Ludwig W, Glöckner FO (2008) A standard operating procedure for  
928 phylogenetic inference (SOPPI) using (rRNA) marker genes. Syst Appl Microbiol 31:251–  
929 257. doi: 10.1016/j.syapm.2008.08.003
- 930 Price MN, Dehal PS, Arkin AP (2010) FastTree 2 — approximately maximum-likelihood trees for  
931 large alignments. PLoS One 5:e9490. doi: 10.1371/journal.pone.0009490
- 932 Pruesse E, Peplies J, Glöckner FO (2012) SINA: accurate high-throughput multiple sequence  
933 alignment of ribosomal RNA genes. Bioinformatics 28:1823–1829. doi:  
934 10.1093/bioinformatics/bts252
- 935 Quast C, Pruesse E, Yilmaz P, et al (2013) The SILVA ribosomal RNA gene database project:  
936 improved data processing and web-based tools. Nucleic Acids Res 41:D590–6. doi:  
937 10.1093/nar/gks1219
- 938 R Core Team (2019) R: A Language and Environment for Statistical Computing. R Foundation for  
939 Statistical Computing, Vienna, Austria
- 940 Rambaut A, Drummond AJ (2009) FigTree version 1.4.3.

- 941 Reva ON, Tümmler B (2004) Global features of sequences of bacterial chromosomes, plasmids  
942 and phages revealed by analysis of oligonucleotide usage patterns. *BMC Bioinformatics*  
943 5:90. doi: 10.1186/1471-2105-5-90
- 944 Richter M, Rosselló-Móra R (2009) Shifting the genomic gold standard for the prokaryotic species  
945 definition. *Proc Natl Acad Sci USA* 106:19126–19131. doi: 10.1073/pnas.0906412106
- 946 Rocha EPC, Danchin A (2002) Base composition bias might result from competition for metabolic  
947 resources. *Trends Genet* 18:291–294. doi: 10.1016/S0168-9525(02)02690-2
- 948 Sabree ZL, Huang CY, Okusu A, et al (2013) The nutrient supplying capabilities of Uzinura, an  
949 endosymbiont of armoured scale insects. *Environ Microbiol* 15:1988–1999. doi:  
950 10.1111/1462-2920.12058
- 951 Saha R, Farrance CE, Verghese B, et al (2013) *Klebsiella michiganensis* sp. nov., a new  
952 bacterium isolated from a tooth brush holder. *Curr Microbiol* 66:72–78. doi:  
953 10.1007/s00284-012-0245-x
- 954 Schloss PD, Westcott SL, Ryabin T, et al (2009) Introducing mothur: open-source, platform-  
955 independent, community-supported software for describing and comparing microbial  
956 communities. *Appl Environ Microbiol* 75:7537–7541. doi: 10.1128/AEM.01541-09
- 957 Shigenobu S, Watanabe H, Hattori M, et al (2000) Genome sequence of the endocellular bacterial  
958 symbiont of aphids *Buchnera* sp. APS. *Nature* 407:81–86. doi: 10.1038/35024074
- 959 Shin SH, Kim S, Kim JY, et al (2012) Complete genome sequence of *Klebsiella oxytoca* KCTC  
960 1686, used in production of 2,3-butanediol. *J Bacteriol* 194:2371–2372. doi:  
961 10.1128/JB.00026-12
- 962 Simão FA, Waterhouse RM, Ioannidis P, et al (2015) BUSCO: assessing genome assembly and  
963 annotation completeness with single-copy orthologs. *Bioinformatics* 31:3210–3212. doi:  
964 10.1093/bioinformatics/btv351
- 965 Simmons JS (1926) A culture medium for differentiating organisms of typhoid-colon aerogenes  
966 groups and for isolation of certain fungi. *J. Infect. Dis.*
- 967 Sinotte VM, Freedman SN, Ugelvig LV, Seid MA (2018) *Camponotus floridanus* ants incur a trade-  
968 off between phenotypic development and pathogen susceptibility from their mutualistic  
969 endosymbiont *Blochmannia*. *Insects*. doi: 10.3390/insects9020058
- 970 Sloan DB, Moran NA (2012) Endosymbiotic bacteria as a source of carotenoids in whiteflies. *Biol*  
971 *Lett* 8:986–989. doi: 10.1098/rsbl.2012.0664
- 972 Sohail M, Latif Z (2016) Phylogenetic analysis of polygalacturonase-producing *Bacillus* and  
973 *Pseudomonas* isolated from plant waste material. *Jundishapur J Microbiol* 9:e28594. doi:  
974 10.5812/jjm.28594
- 975 Stackebrandt E (2006) Taxonomic parameters revisited : tarnished gold standards. *Microbiol*  
976 *Today* 33:152–155.
- 977 Storelli G, Strigini M, Grenier T, et al (2018) *Drosophila* perpetuates nutritional mutualism by  
978 promoting the fitness of its intestinal symbiont *Lactobacillus plantarum*. *Cell Metab* 27:362–  
979 377.e8. doi: 10.1016/j.cmet.2017.11.011
- 980 Takano E (2006) Gamma-butyrolactones: Streptomyces signalling molecules regulating antibiotic  
981 production and differentiation. *Curr Opin Microbiol* 9:287–294. doi:  
982 10.1016/j.mib.2006.04.003
- 983 Tamas I, Klasson L, Canbäck B, et al (2002) 50 million years of genomic stasis in endosymbiotic  
984 bacteria. *Science* 296:2376–2379. doi: 10.1126/science.1071278
- 985 van Ham RCHJ, Kamerbeek J, Palacios C, et al (2003) Reductive genome evolution in *Buchnera*  
986 *aphidicola*. *Proc Natl Acad Sci USA* 100:581–586. doi: 10.1073/pnas.0235981100
- 987 Von Dohlen CD, Moran NA (2000) Molecular data support a rapid radiation of aphids in the  
988 Cretaceous and multiple origins of host alternation. *Biological Journal of the Linnean*  
989 *Society* 71:689–717. doi: 10.1006/bjil.2000.0470
- 990 Wegener CB (2002) Induction of defence responses against Erwinia soft rot by an endogenous  
991 pectate lyase in potatoes. *Physiol Mol Plant Pathol* 60:91–100. doi:  
992 10.1006/pmpp.2002.0377
- 993 Weiss B, Kaltenpoth M (2016) Bacteriome-localized intracellular symbionts in pollen-feeding  
994 beetles of the genus *Dasytes* (Coleoptera, Dasytidae). *Front Microbiol* 7:1486. doi:  
995 10.3389/fmicb.2016.01486
- 996 Whitten M, Dyson P (2017) Gene silencing in non-model insects: Overcoming hurdles using  
997 symbiotic bacteria for trauma-free sustainable delivery of RNA interference: Sustained RNA

- 998 interference in insects mediated by symbiotic bacteria: Applications as a genetic tool and  
999 as a biocide. *Bioessays*. doi: 10.1002/bies.201600247
- 1000 Whitten MMA, Facey PD, Del Sol R, et al (2016) Symbiont-mediated RNA interference in insects.  
1001 *Proc Biol Sci* 283:20160042. doi: 10.1098/rspb.2016.0042
- 1002 Wickham H (2017) Tidyverse: Easily Install and Load the 'Tidyverse.
- 1003 Wixon J (2001) Featured organism: reductive evolution in bacteria: *Buchnera* sp., *Rickettsia*  
1004 *prowazekii* and *Mycobacterium leprae*. *Comp Funct Genomics* 2:44–48. doi:  
1005 10.1002/cfg.70
- 1006 Woruba DN, Morrow JL, Reynolds OL, et al (2019) Diet and irradiation effects on the bacterial  
1007 community composition and structure in the gut of domesticated teneral and mature  
1008 Queensland fruit fly, *Bactrocera tryoni* (Diptera: Tephritidae). *BMC Microbiol* 19:281. doi:  
1009 10.1186/s12866-019-1649-6
- 1010 Wu D, Daugherty SC, Van Aken SE, et al (2006) Metabolic complementarity and genomics of the  
1011 dual bacterial symbiosis of sharpshooters. *PLoS Biol* 4:e188. doi:  
1012 10.1371/journal.pbio.0040188
- 1013 Xie F, Murray JD, Kim J, et al (2012) Legume pectate lyase required for root infection by rhizobia.  
1014 *Proc Natl Acad Sci USA* 109:633–638. doi: 10.1073/pnas.1113992109
- 1015 Yang Z (1994) Maximum likelihood phylogenetic estimation from DNA sequences with variable  
1016 rates over sites: approximate methods. *J Mol Evol* 39:306–314. doi: 10.1007/BF00160154  
1017